UNCLASSIFIED
Security Classification

AD 746500

**DOCUMENT CONTROL DATA - R & D**

(Security classification of title, body of abstract and indexing annotation must be entered when the overall report is classified)

1. ORIGINATING ACTIVITY (Corporate author)

BELL & HOWELL ELECTRONIC MATERIALS DIV.
360 Sierra Madre Villa
Pasadena, California 91109

2a. REPORT SECURITY CLASSIFICATION
UNCLASSIFIED

2b. GROUP

3. REPORT TITLE

DEVELOPMENT OF GaAs INFRARED WINDOW MATERIAL

4. DESCRIPTIVE NOTES (Type of report and inclusive dates)

Final Technical Report, 1 December 1969 through 30 May 1972

5. AUTHOR(S) (First name, middle initial, last name)

Alan G. Thompson

| 6. REPORT DATE | 7a. TOTAL NO. OF PAGES | 7b. NO. OF REFS |
|---|---|---|
| July 1972 | 59 | 27 |

| 8a. CONTRACT OR GRANT NO. | 9a. ORIGINATOR'S REPORT NUMBER(S) |
|---|---|
| N00014-70-C-0132 | --- |
| b. PROJECT NO. DEFENDER | |
| c. | 9b. OTHER REPORT NO(S) (Any other numbers that may be assigned this report) |
| d. | --- |

10. DISTRIBUTION STATEMENT

This document has been approved for public release and sale; its distribution is unlimited.

| 11. SUPPLEMENTARY NOTES | 12. SPONSORING MILITARY ACTIVITY |
|---|---|
| | OFFICE OF NAVAL RESEARCH<br>Physics Branch<br>Arlington, Virginia 22217 |

13. ABSTRACT

The choice of a window material suitable for high power $CO_2$ lasers emitting at 10.6 microns is discussed. Gallium arsenide was chosen as the primary candidate with gallium antimonide being the object of a subsidiary investigation. The preparation of GaAs is discussed at length. The physical, electrical and optical properties of GaAs are also discussed with particular reference to the high-resistivity form which is necessary to reduce free-carrier absorption at 10.6 microns to an acceptable level. The method used to measure the optical absorption coefficient is a calorimetric one making use of a low power $CO_2$ laser. The variation of the optical absorption coefficient with impurities, different dopants, resistivity, laser beam polarization and various growth parameters is examined. Techniques for preparing material in sizes considerably larger than prior state-of-the-art were developed, and included a Czochralski method for single crystal material and both crucible casting and radial casting for polycrystalline material. The latter novel technique shows great potential for an extension to diameters on the order of 25 cm. Finally, some suggestions are made for the lines along which future investigations should proceed in order to elucidate the problems uncovered during the course of this work.



DD FORM 1 NOV 65 1473

UNCLASSIFIED
Security Classification

| 14 KEY WORDS | LINK A | | LINK B | | LINK C | |
|---|---|---|---|---|---|---|
| | ROLE | WT | ROLE | WT | ROLE | WT |
| Semiconductors | | | | | | |
| III-V Compounds | | | | | | |
| Crystal Growth | | | | | | |
| Large Diameter Material | | | | | | |
| Crucible Casting | | | | | | |
| Radial Casting | | | | | | |
| Gallium Arsenide | | | | | | |
| Gallium Antimonide | | | | | | |
| Impurities | | | | | | |
| Electrical Properties | | | | | | |
| Optical Absorption | | | | | | |
| Infrared Windows | | | | | | |
| Carbon Dioxide Lasers | | | | | | |

# DEVELOPMENT OF GaAs INFRARED WINDOW MATERIAL

Final Technical Report

Contract No. N00014-70-C-0132


Prepared by

Alan G. Thompson


Approved by

Robert K. Willardson

Robert K. Willardson, General Manager


BELL & HOWELL ELECTRONIC MATERIALS DIVISION
PASADENA, CALIFORNIA 91109


July 1972



Submitted by

OFFICE OF NAVAL RESEARCH
PHYSICS BRANCH
ARLINGTON, VIRGINIA 22217

This research is part of Project DEFENDER under the joint sponsorship of the Advanced Research Projects Agency, the Office of Naval Research, and the Department of Defense.

The opinions and conclusions expressed in this report are those of the author and are not to be construed as the official policies of either ARPA or the U. S. Government.

## ABSTRACT

The choice of a window material suitable for high power $CO_2$ lasers emitting at 10.6 microns is discussed. Gallium arsenide was chosen as the primary candidate with gallium antimonide being the object of a subsidiary investigation. The preparation of GaAs is discussed at length. The physical, electrical and optical properties of GaAs are also discussed with particular reference to the high-resistivity form which is necessary to reduce free-carrier absorption at 10.6 microns to an acceptable level. The method used to measure the optical absorption coefficient is a calorimetric one making use of a low power $CO_2$ laser. The variation of the optical absorption coefficient with impurities, different dopants, resistivity, laser beam polarization and various growth parameters is examined. Techniques for preparing material in sizes considerably larger than prior state-of-the-art were developed, and included a Czochralski method for single crystal material and both crucible casting and radial casting for polycrystalline material. The latter novel technique shows great potential for an extension to diameters on the order of 25 cm. Finally, some suggestions are made for the lines along which future investigations should proceed in order to elucidate the problems uncovered during the course of this work.

# CONTENTS

# FIGURES

## TABLES

## 1. INTRODUCTION

With the recent development of carbon dioxide lasers emitting at 10.6 microns, particularly those having high power outputs, the selection and fabrication of suitable window materials has become a problem. The classical window materials for this wavelength region are the halide salts, such as sodium chloride or potassium bromide. While the bulk optical absorption coefficients of this class of materials are small, their physical properties leave much to be desired. They are hygroscopic, which leads to high surface optical absorption, soft and difficult to work. At high power levels they suffer from thermal fracture. Non-oxide glasses formed from the heavy elements show much improved physical properties and can be cast in large sizes. However, their absorption coefficients and poor thermal properties lead to thermal runaway and fracture. Semiconductors have excellent physical properties and can be easily worked. Their thermal properties are usually markedly better than either of the above classes of material. Their absorption coefficients are generally higher than those of the halide salts, but lower than those of the chalcogenide glasses. For a more complete discussion of the above problem the reader should consult References 1 and 2.

The major criteria for selecting a suitable semiconductor material are quite easily stated, but the choice inevitably involves a compromise. The material should have very few free carriers at the temperature at which it is to be used--we are assuming here that normal ambient conditions of 300 ± 100°K apply (other materials become suitable at lower temperatures). In order that thermal generation of carriers be small, the fundamental (or lowest) energy band gap should be greater than approximately 0.8 eV. On the other hand the band gap should not be too high for the more covalent semiconductors, since the lighter atoms involved will raise the phonon frequencies to the point where they cause appreciable absorption at 10.6 microns.

For some types of operation a high thermal conductivity is required, and this property gets poorer as the ionicity of the material increases. The physical properties required will depend on the application, but usually the material has to be inert in a variety of atmospheres at normal temperatures and hard so that it may be worked easily. For further discussion on "figures of merit" for different applications the reader is referred to References 1-4.

Of the group IV materials, silicon can be made sufficiently pure that the free-carrier absorption is negligible, but the phonon-bands tail is too large at 10.6μm for laser use. Germanium has been widely used, but has to be cooled due to thermal runaway problems caused by its low energy band gap. Edge cooling of germanium windows leads to problems of thermal gradients and hence variations in refractive index and optical flatness. It also adds considerably to the weight and mechanical complexity of the laser.

Examining the III-V materials it is found that the aluminum compounds and the phosphides have phonon summation bands at too short a wavelength; then only GaSb and GaAs satisfy the band gap criterion. These two have been selected for this study and will be discussed in detail later.

The II-VI materials suffer from poorer thermal conductivity and increased ionicity but candidates such as CdTe and ZnSe have proved excellent for some applications. Unfortunately present II-VI technology is not very well developed, although much work is being done to extend the size of these materials to useful dimensions.

The objective of this work has therefore been to concentrate on GaAs and GaSb, particularly the former since it can be prepared in high resistivity form, and to examine the optical absorption process at 10.6 microns and optimize the material for $CO_2$ laser window use. The development of

material in a size considerably larger than that previously available commercially was also of importance in demonstrating the scale-up potential of GaAs.

The first year's work on this contract has been covered in a Technical Summary Report (December, 1970).[5] This report will include only that material necessary for a meaningful discussion of the second year's work rather than duplicating Reference 5.

## 2. CRYSTAL GROWTH OF GaAs

### 2.1 Sealed System

The equipment used to pull GaAs by the sealed system technique is shown in Figure 1. A full description of the system and the method used for pulling GaAs was given in the previous report[5] and will not be elaborated on here. No ingots were pulled using this technique on the second year's work since it was considered desirable to have reproducibility for certain aspects of the work. Due to the greater mechanical and thermal stability of the liquid encapsulated system it was used for the experiments described below. An additional benefit was the higher yield achieved with the liquid encapsulation technique which resulted in larger ingots.

### 2.2 Liquid Encapsulation System

This system was also briefly described in Reference 5 but will be described in more detail here because certain parameters which were kept constant previously were varied during the course of the second year.

The basic equipment layout is shown in Figure 2. Here the seed rotation and height control is done by mechanical coupling. There is also provision for crucible rotation and height control, but these features were not utilized during the course of this work since an adequate temperature gradient could be maintained during ingot growth. The melt is contained in a crucible and encapsulated in a liquid glass. By maintaining an inert gas pressure in excess of the arsenic pressure at the melting point of GaAs on the liquid glass s iometry can be maintained. This technique was first used by Metz et al[6] to prepare PbSe and PbTe and was later applied to other m erials.[7,8]

Pieces of GaAs are loaded into the quartz crucible and a slug of the encapsulant placed on top of the GaAs. The encapsulant used here was boric oxide, which was prepared by heating boric acid in a platinum crucible for

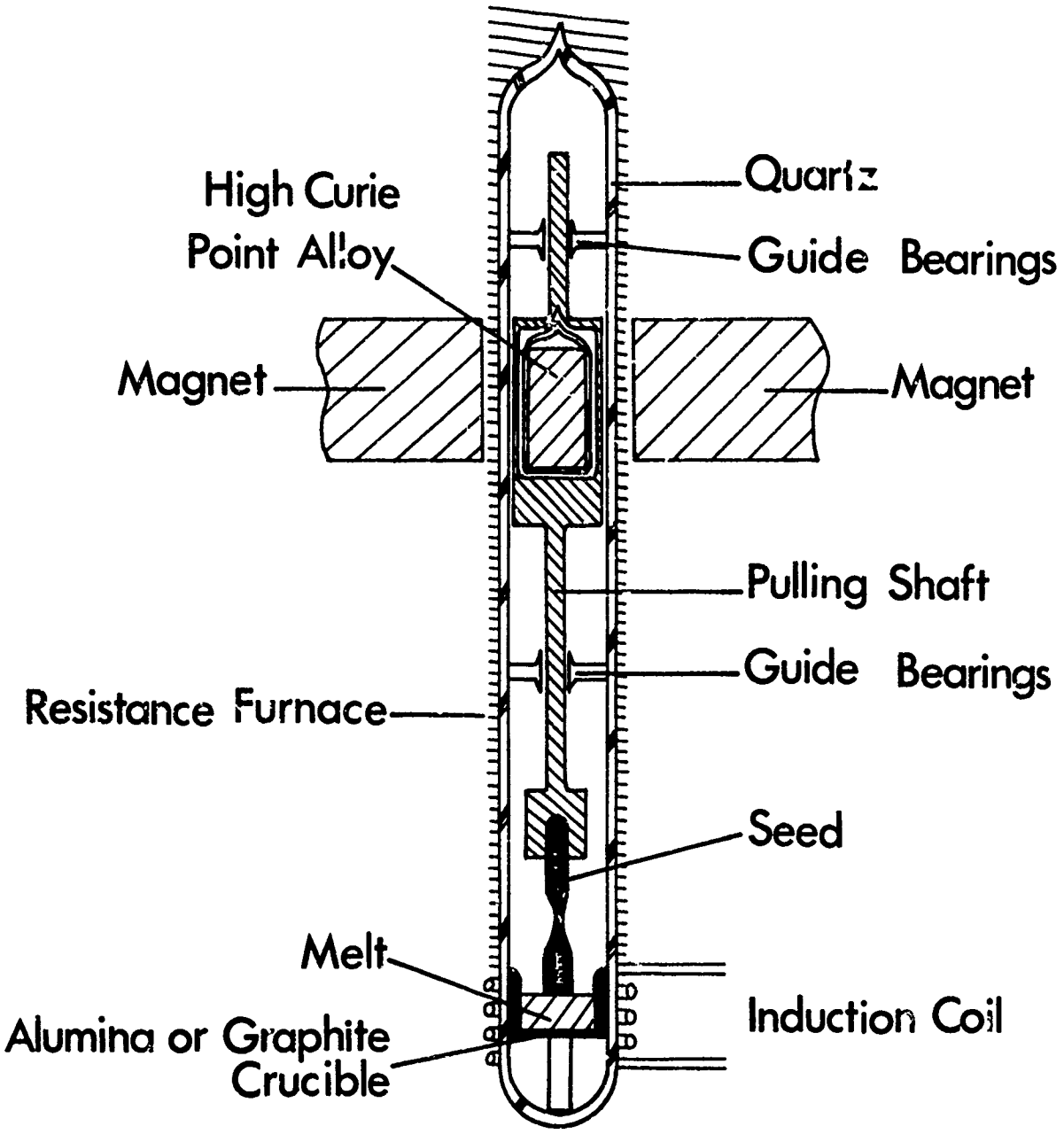


Figure 1. Diagram of Apparatus Used for Pulling Crystals by the Sealed Czochralski Technique

several days at 1,000 °C. After pumping and flushing the chamber the boric oxide is melted and baked out under vacuum to remove as much water as possible. If this is not done it turns opaque during crystal growth and prevents viewing of the solid-liquid interface. The heater is ther removed and the RF coil is positioned correctly. The RF power is then turned on and coupled to the graphite susceptor which heats the melt. At the same time the chamber is pressurized to about two atmospheres with high-purity nitrogen. When the melting point of GaAs has been exceeded by 20 or 30 °C, the melt is allowed to homogenize for an hour or so before growth is commenced in the usual manner.

Typical ingots had diameters of 3-4 cm and lengths of 5-10 cm, but some ingots were deliberately kept small in diameter and long in order to examine some of the growth parameter effects on the absorption coefficient. Pull speeds ranged from 0.5 to 2.5 cm $hr^{-1}$ for stoichiometric melts while a constant rotation speed of 6 rev $min^{-1}$ was used. Growth orientations tried were <111>A and B, <110>, <100>, <311>A and B and <511>A. The dopant used in all cases was Cr with the same amount usually being added to a (constant-size) melt. Some conclusions on segregation coefficients appear in the next section. Other dopants were tried previously, but did not appear promising.[5]

Ingots were also grown from non-stoichiometric melts ranging from 45 to 30% Ga. A growth orientation of <111>A was used throughout this portion of the program. Single crystals were obtained out to and including the 30% Ga composition, and ingot sizes ranged down to 40 grams and 1.5 cm diameter. No attempts were made to optimize the thermal gradients for the different compositions, that normally used for <111>A pulls from stoichiometric melts being utilized. Growth speeds as low as 0.3 cm $hr^{-1}$ were found necessary to prevent the ingot from going polycrystalline and/or the occurrence of gallium inclusions.

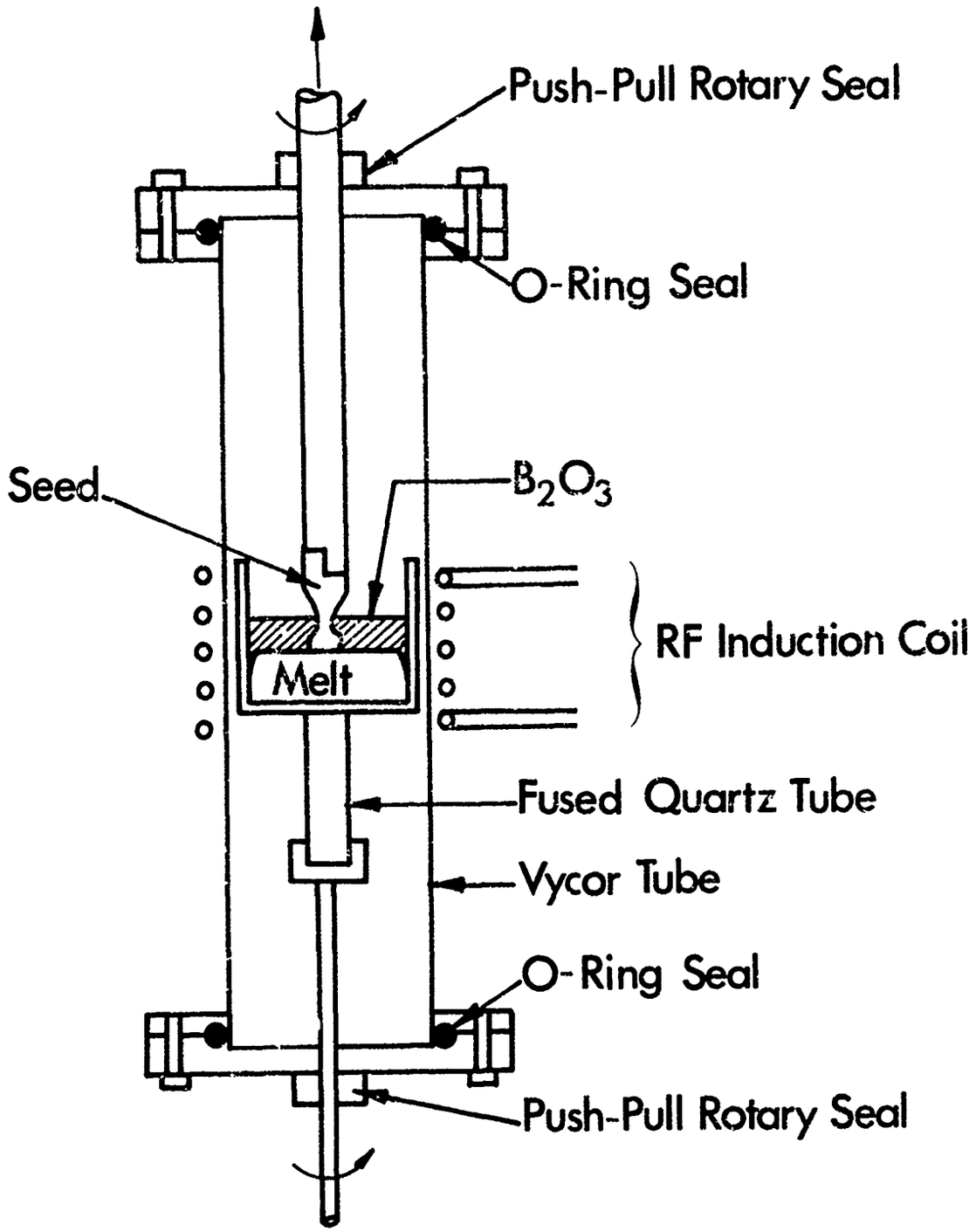


Figure 2. Diagram of Apparatus Used for Pulling Crystals by the Czochralski Technique Under $B_2O_3$ Glass

It is believed that this is the first published report of successful growth of bulk single crystals of GaAs from grossly non-stoichiometric melts, although other semiconducting materials (e.g. GaP,[9] $InAs_{1-x}P_x$[10] and $Pb_{1-x}Sn_xTe$[11]) have been prepared in this way in order to facilitate their growth or modify their properties.

# 3. PHYSICAL AND ELECTRICAL PROPERTIES

## 3.1 Semi-insulating GaAs

Relatively uncompensated GaAs grown from stoichiometric melts typically contains one to two ppma of electrically-active impurities, corresponding to an n-type carrier concentration in the low $10^{16} cm^{-3}$ region. However, certain dopants have been shown to be capable of reducing this carrier concentration by orders of magnitude, yielding room temperature resistivities from $10^3$ to $10^8$ ohm-cm, the latter being close to the calculated intrinsic value for GaAs. The dopants which have commonly been used are the transition metals such as iron, cobalt and nickel and other elements including chromium, oxygen, copper and zinc. A brief bibliography of this work is given in References 12 and 13. Most of these elements apparently give one or more deep levels, with zinc being the exception. It gives a shallow acceptor and the amount needed to compensate the shallow donors is very critical; this mechanism is assisted by the small amounts of chromium, iron, etc., which are usually present in GaAs.

The accepted mechanism for the semi-insulating state is based on a model originally proposed by Blanc and Weisberg.[14] They suggested shallow donor and acceptor levels close to the conduction and valence band edges respectively and a deep donor close to the center of the energy gap. If this deep donor is replaced by a deep acceptor the observation of both n- and p-type semi-insulating material can be explained without the need for close compensation. Figure 3 shows the proposed energy band diagram for GaAs at $\underline{k} = 0$. With this model the number of deep acceptor impurities only has to exceed $(N_D - N_A)$ to give essentially intrinsic behavior.

## 3.2 Physical Properties of GaAs

The GaAs ingots grown by both the sealed system technique and the liquid encapsulation technique were evaluated for crystallinity and dislocation

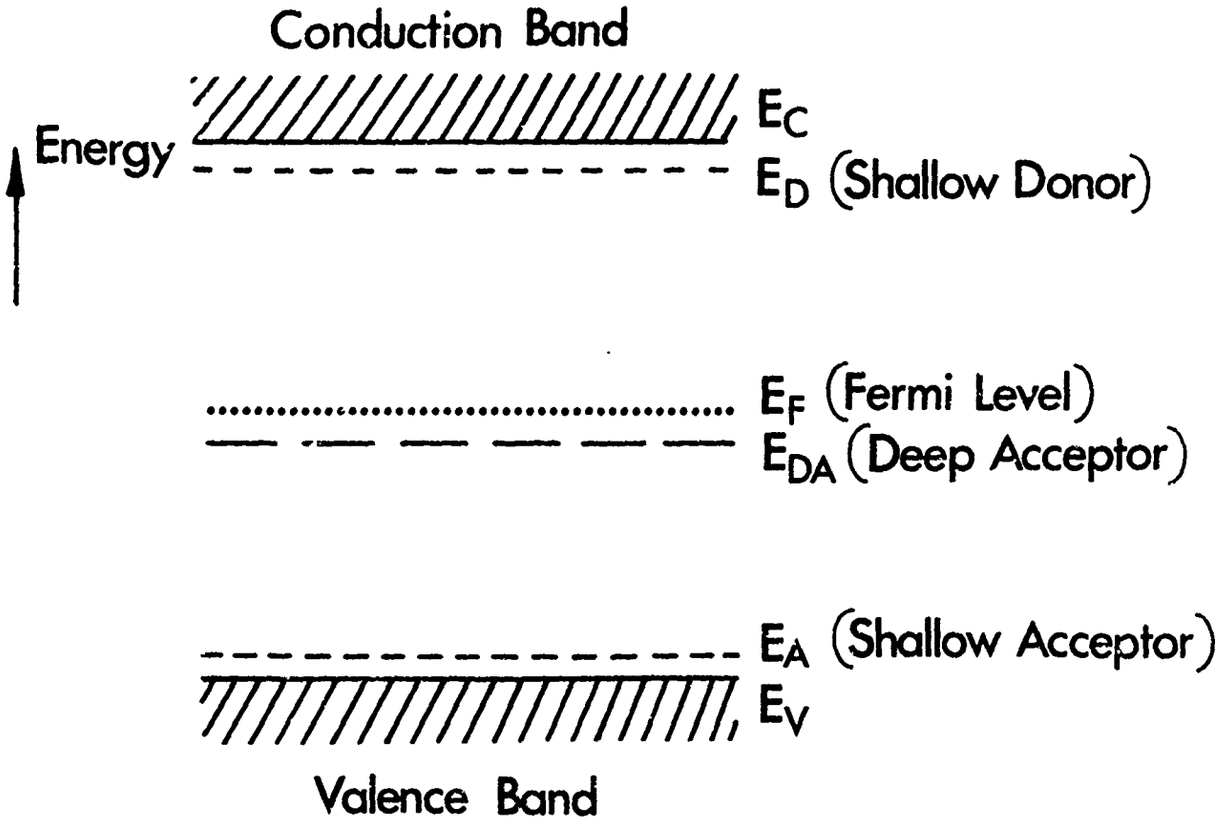


Figure 3. Energy Levels at k=0 in Semi-insulating GaAs, According to a Modified Blanc-Weisberg Model[14] and Experiment[13]

density. Evaluation slices were cut from just below the crown and the bottom of the single crystal portion of the ingot. These were lapped, chemically polished ($HF:HNO_3:H_2O$, 1:3:4; two minutes) and etched to reveal dislocations ($HNO_3:H_2O$, 1:2, three minutes). The counting of dislocations was done in five different areas and any tendency toward lineage or grain boundaries noted. The crystals grown by the sealed system technique typically contained $\sim 10^4\ cm^{-2}$ at the top and $\sim 10^5\ cm^{-2}$ at the bottom. The liquid encapsulation crystals were lower on average by half an order of magnitude. Only material without noticeable patterns of dislocations was used for the optical measurements. In all, about thirty ingots of GaAs yielded material of sufficiently high quality for the electrical and optical measurements during the second year of this program.

### 3.3 Impurities in GaAs

The evaluation slices described above were used to provide Hall bars (see next sub-section) and small bars for spark source mass spectrometric analysis. The latter were usually lapped, degreased and etched (in $HNO_3:HF:H_2O$, 1:1:1) sufficiently to remove an appreciable amount of material. Clean procedures were followed until the loading of the mass spectrometer was complete. The instrument used (a modified CEC X21-110) has ion pumping with adequate cold-trapping. All elements were examined, and a summary of the results is shown in Table 1.

The numbers given for both detection limits and concentrations are on the conservative side, i.e., $< 0.1$ ppma indicates that in most samples the measured value was $\leq 0.05$ ppma, a few samples contained 0.05-0.10 ppma and occasionally a level slightly above 0.1 ppma was seen. Samples cut from both tops and bottoms of ingots are included and the survey covers over sixty analyses. A special technique was developed for sodium which normally is obscured by the triply-ionized gallium line. The levels observed are in general similar to those reported previously but with some elements being

TABLE 1

Summary of Mass Spectrometric Analyses of
Impurities Present in Cr-doped Liquid Encapsulated GaAs

| Element | Typical Detection Limit ppma | Average Concentration ppma |
|---|---|---|
| Li | 0.01 | < 0.1 |
| B | 0.05 | 0.25 |
| C | 0.05 | 1.3 |
| N | 0.05* | < 0.1 |
| O | 0.05* | 2.4 |
| F | 0.05 | < 0.1 |
| Na | 0.5 | 2.0 |
| Al | 0.1 | 0.6 |
| Si | 0.05 | 0.3 |
| P | 0.05 | < 0.2 |
| S | 0.1 | 1.4 |
| Cl | 0.1 | < 0.1 |
| K | 0.1 | < 0.5 |
| Ca | 0.05 | < 0.1 |
| Cr | 0.1 | 3.5 |
| Fe | 0.1 | < 0.5 |
| Ni | 0.1 | < 0.5 |
| Cu | 0.05 | < 0.1 |
| Zn | 0.1 | < 0.1 |

Notes: All other elements were not detected with detection limits of approximately 0.2 ppma.

* Plate sensitivity, does not take into account outgassing of instrument, oxidized surfaces, etc.

lower which is probably due to improved material handling techniques and a much greater experience with Cr-doped liquid encapsulated GaAs.

It is believed that some of the C, N, O, F and Cl comes from the cleaning and handling procedures and residuals in the instrument. The Na has a distribution coefficient greater than unity (probably $\sim 3$) and hence appeared only in the first-to-grow portions of the ingots. The Al is traceable to the GaAs starting material used which acquired it from the gallium and through the use of alumina crucibles; the level in the liquid encapsulated material is appreciably lower than was observed in the sealed system material.[5] The Si and S are both present in the charge material which acquired them from the elemental As and reactions with the silicon pulling chamber. Chromium was, of course, the intentional dopant, while the Fe and Ni were previously observed to associate themselves with Cr and had their origins in the elemental As and possibly Ga.

The distribution coefficients of the various impurities that were present at measurable levels checked with those reported in the literature.[5, 15] It was found however, that although the value for Cr was constant for ingots grown on the <111>A and B, <110> and <311>, a level ~50% higher on average was found for ingots grown on the <100>. Average levels at the tops of ingots were $2.0 \pm 0.5$ ppma for all except the <100> which contained $3.2 \pm 0.5$ ppma. Thus the values for Cr in GaAs are

$k_o$ (Cr) = $6.0 \times 10^{-4}$ for the <110>, <111> and <311> orientations
$k_o$ (Cr) = $1.0 \times 10^{-3}$ for the <100> orientation.

No significant deviations were found for growth spreads in the range of 0.5 to 2.5 cm hour$^{-1}$. Insufficient data were available to draw any conclusions on the segregation coefficient for Cr in the <511> growth direction.

The ingots grown from non-stoichiometric melts showed generally

decreasing total impurity contents as would be expected. Only in these ingots did the distribution coefficient for Cr show signs of increasing, but the results were inadequate statistically to permit a quantitative conclusion.

## 3.4 Chromium Segregation in GaAs

It was previously pointed out[5] that a search was made to detect the segregation of chromium and other impurities on a microscopic scale, but that no evidence for segregation within the spatial resolution ($\sim 1\mu$) of the instrument, a CAMECA/Bell & Howell Direct Imaging Mass Analyzer. A few samples were also examined by infrared microscopy in the 0.9-1.1 micrometer wavelength region, but no evidence for clumps or vacancies or chromium on a large scale could be found, again within the instrument resolution ($\sim 1\mu$).

It has been suggested[5, 18] that chromium may segregate due to its very low distribution coefficient (compared to the other commonly used dopants for example) and form complexes on a sub-micron scale. Jungbluth[18] has given a comprehensive review of this and other types of defect in GaAs. Under a parallel contract[19] to this work, the A. D. Little Company is performing analyses on our material by a variety of techniques in an effort to determine if such sub-micron defects are present. At the time of writing their work had not progressed to the stage where any conclusions could be made.

## 3.5 Electrical Properties of Semi-insulating GaAs

Resistivity measurements were made on ultrasonically cut bridge-shaped samples. After thorough cleaning the samples were contacted with indium in a reducing atmosphere at 450 °C for one to two minutes. After soldering wires to the contacts the sample was degreased and placed in a light-proof holder. The measurement was performed with a teraohmmeter. Although the accuracy of this method is not very good, it is adequate since

resistivities ranging from $10^3$ to $10^8$ ohm-cm were found. All electrical measurements were done at room temperature.

As previously found, most of the Cr-doped ingots exhibited resistivities between $10^6$ and $10^8$ ohm-cm, with the latter corresponding to the heavier doped material. At the lower doping levels the resistivity would revert very quickly to normal "undoped" levels if the amount of chromium were insufficient to overcome the net donor density. Thus approximately one ppma of chromium was usually required in order to yield high-resistivity material.

No Hall measurements were made on these materials. Other workers have reported quite widely varying results, with carrier concentrations between $10^7$ and $10^{11}$ $cm^{-3}$ and mobilities of 10-1,000 $cm^2 V^{-1} sec^{-1}$ (see for example References 12, 16, and 17). One clue to these discrepancies is the rapid change in Hall coefficient and mobility with temperature[17] around 290 °K. Because a resistivity exceeding $10^6$ ohm-cm suffices to reduce free carrier absorption to negligible limits (see next section) we made no attempts to refine our resistivity measuring system or pursue Hall techniques. However, in view of the discrepancies pointed out above this would seem to be a field where further measurements would be fruitful.

# 4. OPTICAL PROPERTIES

## 4.1 Optical Properties of GaAs

The optical properties of GaAs have been well documented at energies above, close to and below the fundamental gap (see chapters 2, 4, 5, 6 and 9 of Reference 20). In the region of interest, close to 10.6 microns, the properties have only been examined in detail for samples having free carrier absorption. Thus Cochran et al[17] show an absorption coefficient that is essentially zero (on their scale) up to 12 microns for a high resistivity sample of GaAs. However with conventional techniques and thin samples absorption coefficients in the 0.01 $cm^{-1}$ range are very difficult to measure absolutely. In the next sub-section we discuss this problem further.

Several reasons have been advanced attempting to explain the small ($\sim$0.01 $cm^{-1}$) residual absorption coefficient at 10.6 microns in GaAs in which free-carrier absorption is negligible. The presence of multiphonon bands in the general region has been shown[17,18] but their magnitude at 10.6 microns is probably small since the three-phonon bands occur at longer wavelengths and the four-phonon bands at shorter wavelengths. Klein and Rudko[19] use a homological argument to suggest that a fourth-order electric moment could give an absorption approximately 0.03 $cm^{-1}$ in GaAs at 10.6 microns. Nicolai and Gottlieb[20] postulate a coupled mode involving the electronic polarizability of the material based on measurements on a variety of materials. An excellent general account covering the physical processes responsible for optical absorption in this wavelength region has been Sparks.[22] The resolution of these arguments depends on accurate measurements of the optical absorption coefficient in pure materials over a spectral range, rather than at one wavelength for a specific purpose as is being done here.[22]

The effects of free carriers may be readily calculated since absorption data on doped GaAs are well documented. Using the results summarized by

Fan (Chapter 9 of Reference 16), the absorption coefficient $\alpha$ is given by

$$\alpha = \sigma_n \cdot n$$

where $\sigma_n$ is proportional to the wavelength raised to a power k. For GaAs at 10.6 microns and 300°K we obtain an $\alpha = 10^{-3}$ $cm^{-1}$ for $n = 1.3 \times 10^{13}$ $cm^{-3}$. Assuming the mobility of high resistivity material in this carrier concentration range is approximately 100 $cm^2V^{-1}sec^{-1}$ or greater[16,17] this is equivalent to a resistivity of approximately $6 \times 10^3$ ohm-cm or less.

Therefore, if the resistivity of GaAs exceeds approximately $10^4$ ohm-cm the additional optical absorption due to free carriers will be negligible compared with the absorption coefficient due to other causes (which is on the order of 0.01 $cm^{-1}$). In Section 4.3 curves are presented showing the variation of $\alpha$ (free carriers) with resistivity.

## 4.2 Measurement of Optical Absorption Coefficient

The technique chosen here to measure the optical absorption coefficient of semiconductors at 10.6 microns is a calorimetric one. This method lends itself to the measurement of small absorption coefficients (in the $10^{-3}$ to $10^{-1}$ $cm^{-1}$ range) with reasonable precision and is quick to perform both from sample preparation and actual measurement points of view. Another advantage is the fact that a $CO_2$ laser is used for the measurement at the same wavelength that the material will be used for windows.

Although many workers in this field have used the so-called adiabatic technique in which the sample is thermally isolated from its surroundings we have chosen to pursue the calibrated loss type of measurement where the sample is connected to an isothermal sink through a conductor. This technique is more rapid than the adiabatic method and is well suited to the measurement of a large number of samples. The excellent thermal conductivity of GaAs results in a reasonable accuracy in spite of variations in sample

size. Further discussion of the accuracy of the technique appears later in this section.

The apparatus used is shown schematically in Figure 4. A Sylvania Model 941 frequency stabilized $CO_2$ laser gives an approximately parallel 5mm diameter beam of 3 to 5 watts at a wavelength of 10.6 microns. The light passes through the sample and is detected and measured by a Coherent Radiation Model 201 power meter. Not shown in Figure 4 in order to aid clarity are stops and an optional polarizer. The sample sits on a plate on top of a brass post.[23] Thermocouples are mounted at the upper and lower ends of the post, the base of which is soldered into a large copper block. Two small carbon resistors are mounted in good thermal contact with the lower side of a thin plate soldered to the top of the post. Thin, long wires carry the current to these resistors. This assembly is contained in a die-cast aluminum box which is painted black inside, and shown as the "sample chamber" in Figure 4. This is mounted in turn on a positioning mechanism so that the sample may be moved up and down and across the laser beam; this was used to check sample homogeneity.

Most of the samples used were cut perpendicular to the growth direction of the ingot and were therefore approximately circular. The sides were lapped parallel and mechanically polished, finished thicknesses falling in the range of 0.4 to 0.8 cm. A ground flat on the edge of the disc was used to mount the sample, aided by a smear of silicone thermal grease. A more extensive discussion on the sample preparation techniques essayed is contained in sub-section 4.3.

After allowing the laser to warm up and stabilize the beam is allowed to fall on the sample. The temperature difference along the post is monitored at frequent intervals until it stabilizes. At that time the reading is noted, the beam blocked and the power to two resistors mounted on the platform turned on. This power is adjusted until the temperature difference is stable

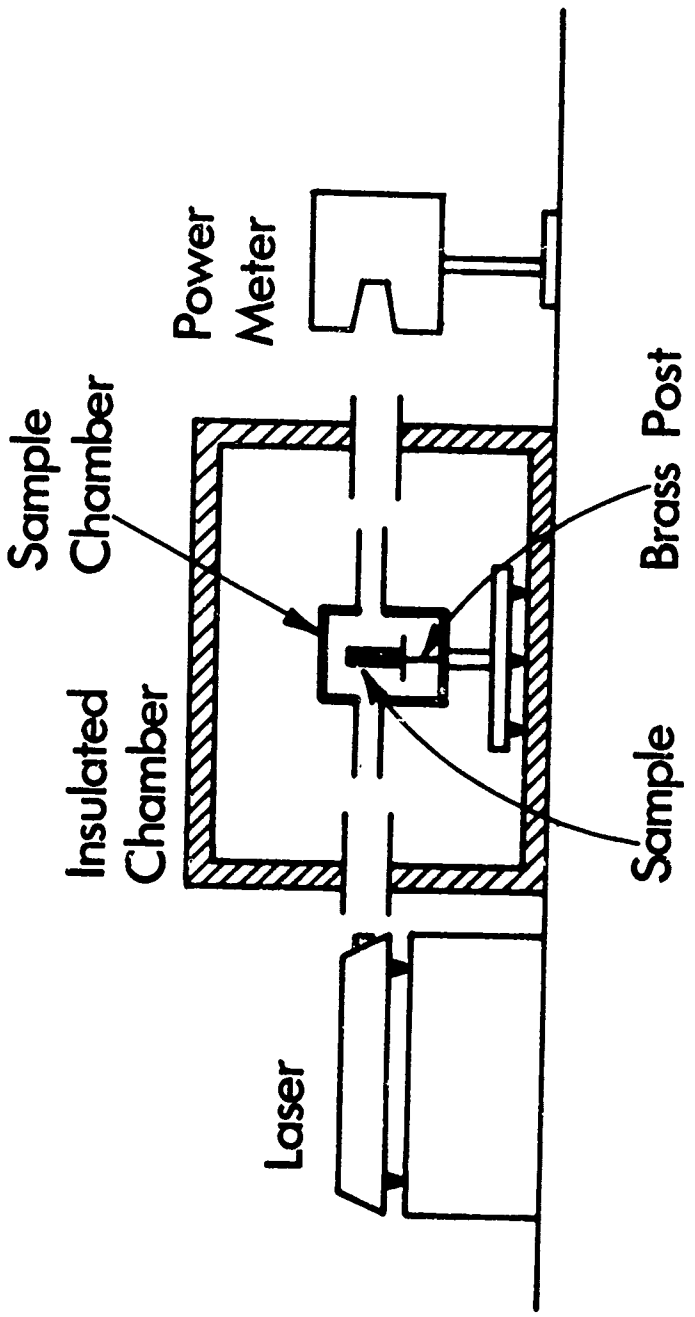


Figure 4. Experimental Arrangement for the Calorimetric Measurement of Optical Absorption Coefficients

and equal to that caused by the laser. The knowledge of this power ($P_s$), the power transmitted by the sample ($P_T$) and the thickness ($\ell$) of the specimen is sufficient to calculate the optical absorption coefficient $\alpha$ of the material using the formula[24]

$$\alpha = \left(\frac{P_s}{\ell P_T}\right)\left(\frac{2n}{n^2+1}\right)$$

For GaAs we have taken n = 3.30, although values reported in the literature range from 3.1 to 3.5. The absolute error introduced by this assumption can be no greater than ±5%. Other errors due to different radiation losses from sample heating and resistor heating, power measurement and so on could run up to ±30%. The relative accuracy for our equipment bearing in mind the sample sizes is approximately ±10% (see next section). If the sample is wedge-shaped, poorly aligned or in poor thermal contact with the platform a higher value of $\alpha$ will generally result. Temperature differentials of less than 1°C were always used with more typical values being 0.2 - 0.4°C. This reduces radiation losses to a negligible level compared to the conduction loss through the post, and minimizes the effects of varying sample size and surface treatment.

## 4.3 Results

Approximately 50 samples have been measured for optical absorption at 10.6μm during this reporting period. Most of these were discs cut from ingots and had approximately circular faces as described earlier in this section. As had been observed previously[5] most of the samples had absorption coefficients between 0.01 and 0.02 $cm^{-1}$ with a few slightly below 0.01 $cm^{-1}$ and several between 0.02 and 0.03 $cm^{-1}$. Those samples exhibiting absorption coefficients greater than 0.03 $cm^{-1}$ were usually imperfect in a crystalline sense, i.e. they had severe lineage, gallium inclusions, etc. due to excessive growth rates or loss of arsenic pressure.

Figure 5 shows the absorption coefficient at 10.6 μm for GaAs doped

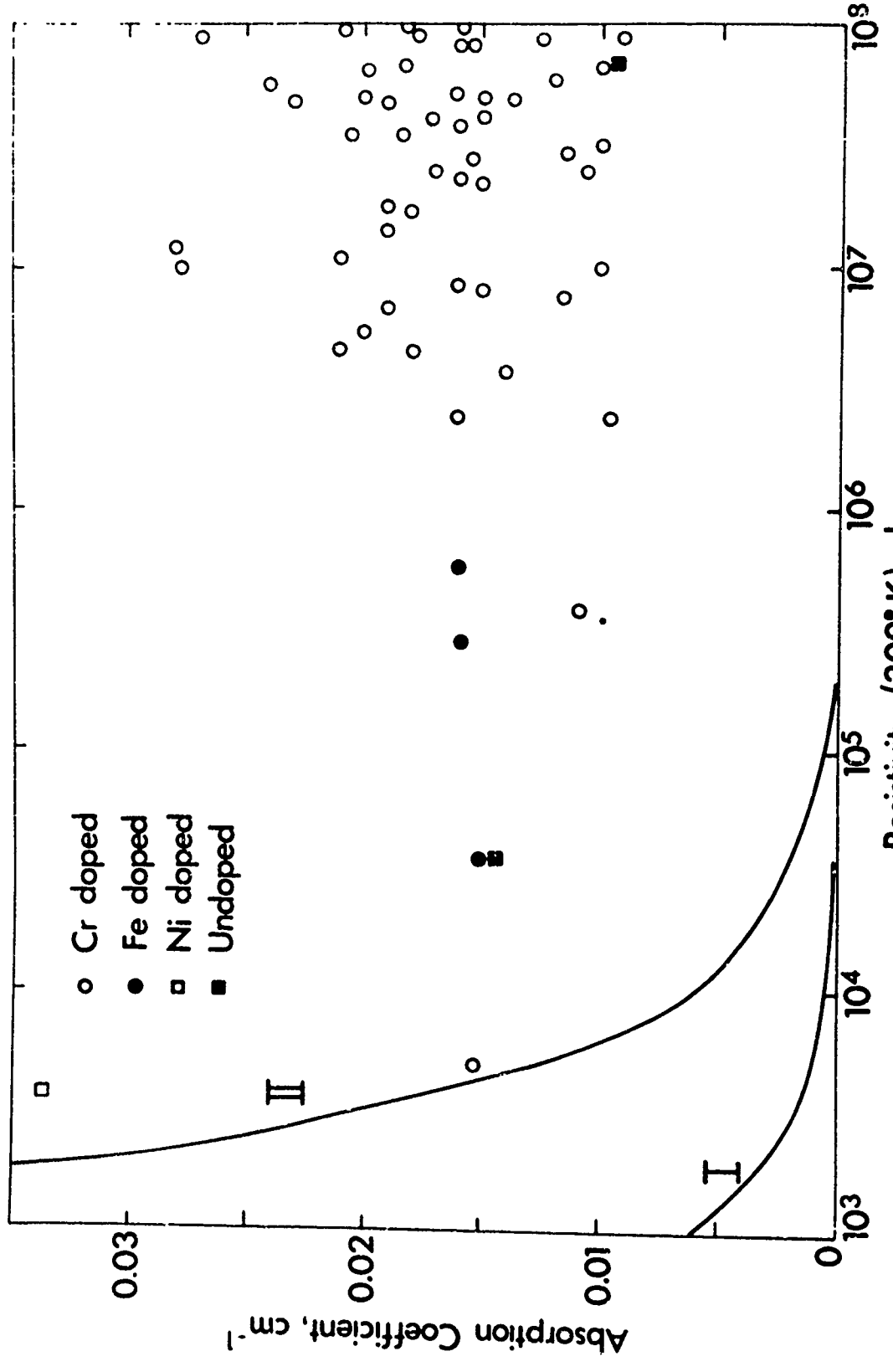


Figure 5. Absorption Coefficient of GaAs as a Function of Resistivity. For explanation of solid lines, see text.

with Cr, Fe, Ni and "undoped" as a function of the room temperature resistivity. Material grown by both the sealed system and by liquid encapsulation has been included in this Figure; results from tops and bottoms of ingots have not been differentiated since no significant differences were apparent. The "undoped" sample shown was grown by liquid encapsulation from an undoped melt with no additional dopant. Although the resistivity was $7 \times 10^7$ ohm-cm at the top it fell to $3.6 \times 10^4$ ohm-cm at the bottom of a small ingot. A mass spectrometric analysis revealed exceptionally low S + Si, a trace of Zn and a high oxygen content. This ingot was therefore high resistivity due to Zn compensation and some oxygen doping. Attempts to reproduce this ingot have been unsuccessful in that either low resistivities were obtained or sufficient Cr + Fe was present for the normal deep level behaviour to occur.

The two solid curves shown in Figure 5 are the theoretical additional contribution to the absorption coefficient at 10.6μm due to free-carrier absorption. The constants used in sub-section 4.1 were assumed to apply in this (higher resistivity) region. Curve I assumes a mobility of 100 $cm^2 V^{-1}sec^{-1}$ while curve II assumes a mobility of 10 $cm^2V^{-1}Sec^{-1}$. For additional information on these assumptions see Section 3.5 and References 16 and 17. Curve I is probably the most realistic one and fits well with the few data we have in this intermediate resistivity range. The graph does stress the insignificance of free-carrier absorption in GaAs for material having a resistivity exceeding $10^6$ ohm-cm

As found previously[5] there was little variation in absorption coefficient along an ingot except in those cases where the bottom had gross crystalline defects. Attempts to correlate the absorption coefficient with dislocation density were fruitless in spite of a two-order of magnitude change in the latter.

The effects of surface treatment were examined closely. The normal processing consisted of cutting the ingot with an o.d. high speed diamond

blade, which causes a considerable amount of damage below the surface. The resulting slab was lapped on a glass plate with 1200 grit grinding compound until the saw marks were entirely removed, then lapped with 3200 grit compound and finally polished on a silk cloth covered wheel with alumina powders down to 0.3μ particle size. The polish was judged adequate when it had a mirror-like finish but there were usually some fine scratches present.

In order to test the adequacy of the above treatment several tests were performed.

(a) A typical sample was prepared in the normal manner as indicated above. Mean $\alpha = 0.0153\ cm^{-1}$.

(b) The same sample was then etched ($HF:HNO_3:H_2O$, 4:3:1) until 50μ had been removed from both surfaces. This should have removed all the work damage from sawing and subsequent lapping. It was then lightly relapped with 3200 grit compound and mechanically polished on the wheel. Mean $\alpha = 0.0138\ cm^{-1}$.

(c) The same sample was chemically polished on both sides with a proprietary process; this removed another 50μ and left both sides essentially damage-free (removing work damage from step (b) ). Mean $\alpha = 0.0147\ cm^{-1}$.

(d) Two samples were cut from another ingot, one by the normal procedure and one using a wire saw with a very light pressure. The normal lapping and polishing were done on both. Mean $\alpha$ (o.d. saw) $= 0.0197\ cm^{-1}$. Mean $\alpha$ (wire saw) $= 0.0185\ cm^{-1}$

The results from the above experiments indicate that work damage from our normal sample preparation treatment is not severe enough to affect the optical absorption coefficient within the reproducibility and accuracy of our equipment.

The effects of chromium concentration on the 10.6 μm absorption

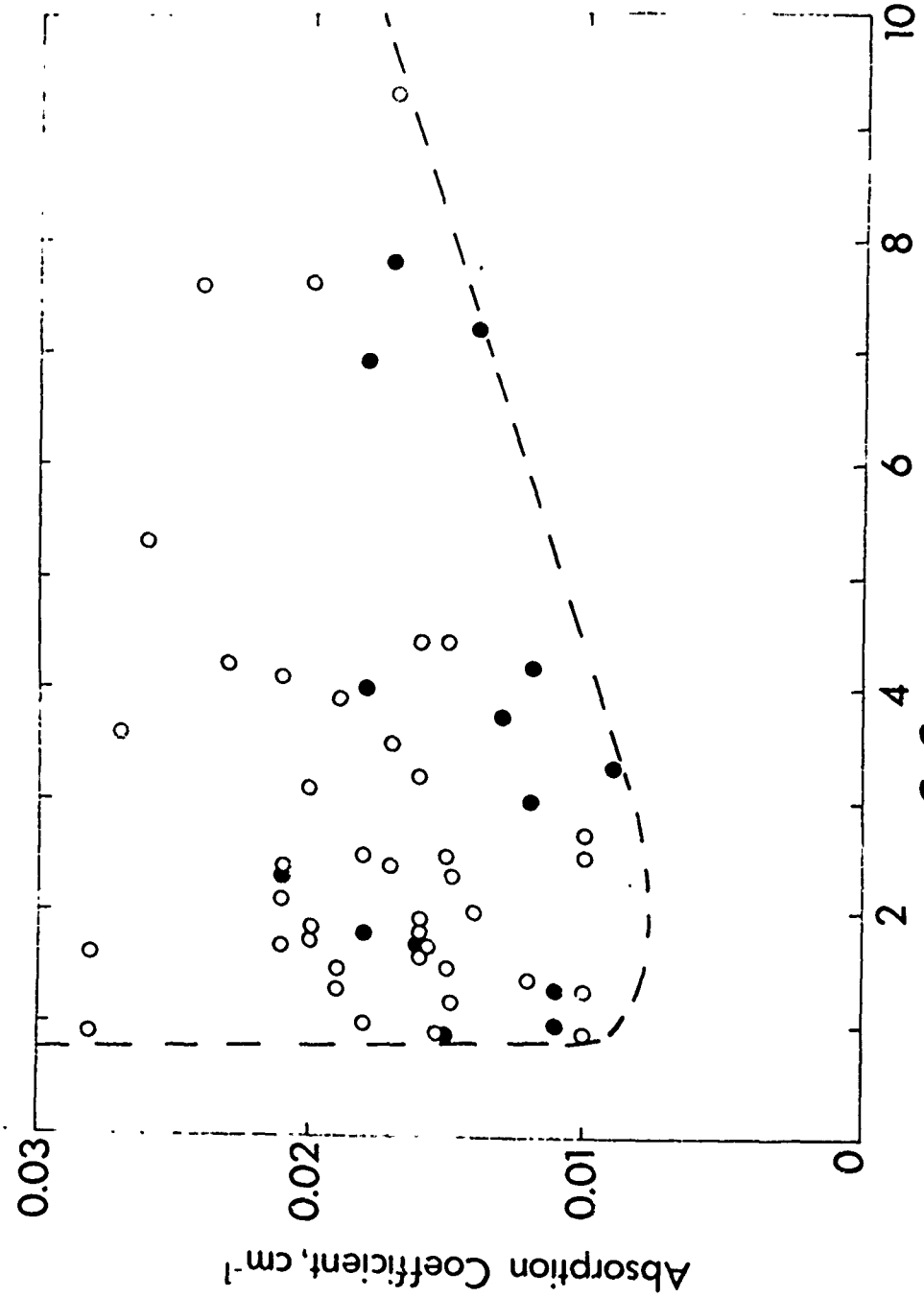


Figure 6: Absorption Coefficient in $cm^{-1}$ as a Function of Cr Content for Sealed System (●) and Liquid Encapsulation (○) GaAs

coefficient are shown in Figure 6. This graph shows a broad minimum for Cr contents between 1 and 4 ppma. Higher concentrations result in higher absorption coefficients possibly due to impurity precipitation (see sub-section 3.4) while lower concentrations result in low resistivity material. It can be seen that for a given Cr content the absorption coefficient can vary by a factor of ~ 3. The dashed line merely indicates an envelope and it is obvious that other parameters are affecting the absorption coefficient more drastically.

In sub-section 2.1 it was stated that attempts were made to pull ingots at a variety of pull speeds and orientations. For the <100>, <110>, <111>A and B and <311>A directions ingots were pulled at speeds of 1.2, 1.8 and 2.4 cm $hr^{-1}$ successfully, although at the highest of these speeds for the <100> and <110> orientations the ingots exhibited polycrystallinity, lineage and gallium inclusions at the bottom resulting in low single crystal yields. The highest absorption coefficients were generally observed at the highest speeds and when gross crystalline defects were present. However, attempts to plot absorption coefficient as a function of growth speed and/or orientation revealed no discernible trends other than that mentioned above. It should be noted that due to the great variety of growth conditions utilized very few duplicate attempts to establish reproducibility were made and hence the statistical significance is poor. The wide range of absorption coefficient for a given Cr concentration only serves to possibly mask any growth speed or orientation dependence.

Ingots were successfully pulled in the <111>A direction from melts ranging from 50% Ga to 70% Ga. These ingots were generally small but provided enough material for an optical sample which therefore corresponded to the first-to-freeze portion (or top) of larger ingots. Two attempts to obtain semi-insulating material from 70% Ga melts were unsuccessful in spite of increasing the chromium doping level. This is not understood since both ingots appeared to have excellent purity and an adequate Cr level. Time did not

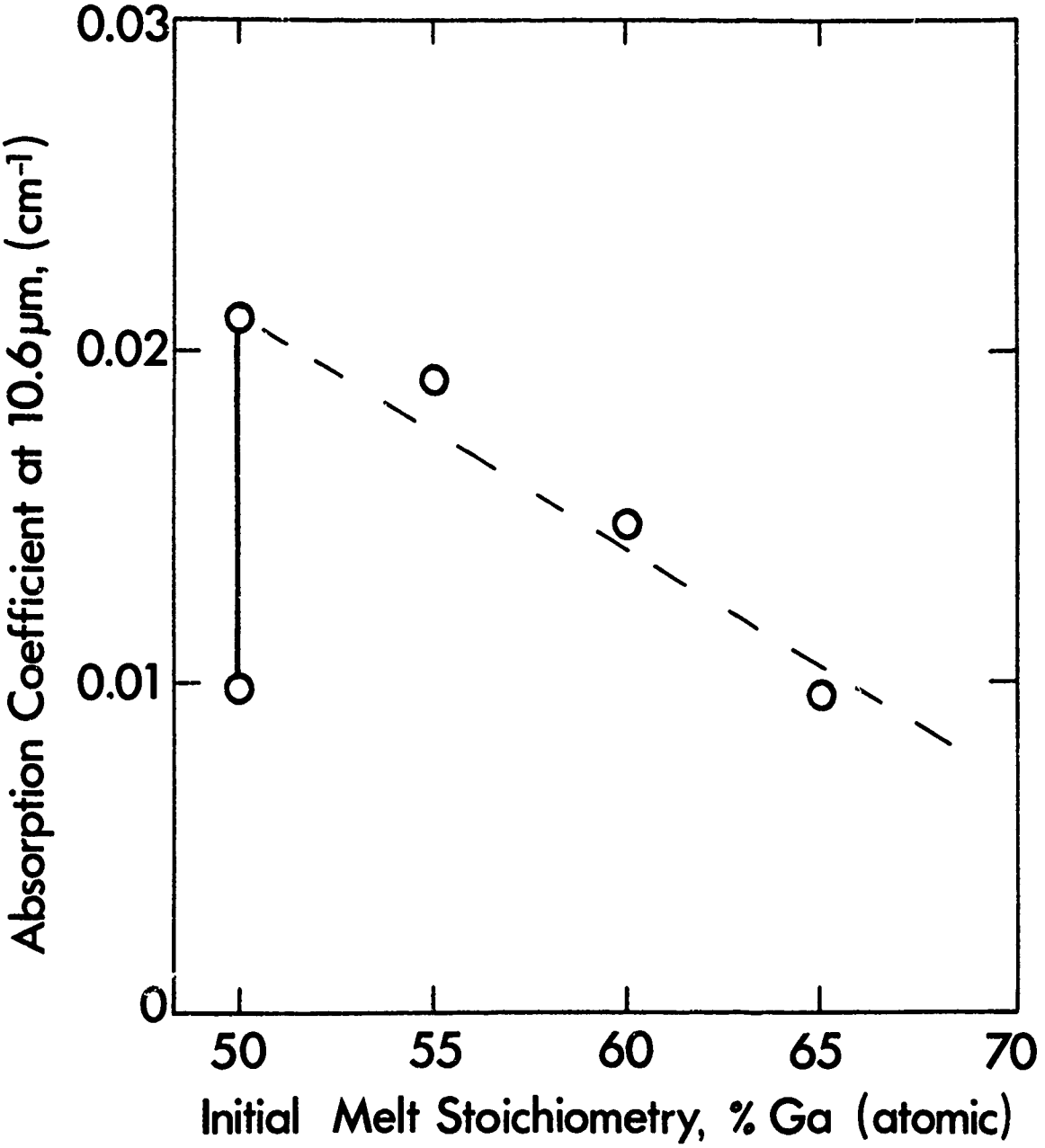


Figure 7. The Absorption Coefficient at 10.6 μm as a Function of Initial Melt Stoichiometry (the range of values shown at 50% Ga are for <111>A ingot tops, at a variety of speeds)

permit a deeper investigation of this effect. The other ingots showed a steadily decreasing absorption coefficient, as shown in Figure 7. However the best ingot pulled from a non-stoichiometric melt had an absorption coefficient comparable with the best <111>A ingot pulled at 1.8 cm $hr^{-1}$ from a stoichiometric melt. Again, time did not permit an extension of this effort but this trend may well prove to be significant.

The effect of impurities on the absorption coefficient has been discussed previously (see sub-section 3.3 and Reference 5). At the levels encountered we could not find any correlation between either type or quantity of any of the impurities looked at and the absorption coefficient. The great majority of the ingots pulled at reasonable speeds with an average Cr concentration exhibited absorption coefficients lying between 0.01 and 0.02 $cm^{-1}$. Ingots in this range exhibited widely varying total impurity content with no apparent correlation between it and the absorption coefficient.

## 4.4 Polarization Effects

Nicolai has suggested[25] that optical absorption at 10.6 μm in some types of crystals can occur via ionic dipole-dipole interactions. This mechanism would manifest itself via the absorption coefficient having a polarization dependence for certain crystallographic orientations. In order to test this theory a Ge Brewster plate polarizer was obtained, since our laser has a randomly polarized output. The power falling on the sample was reduced by this from the 3 to 5 watt range down to 1 to 3 watts, varying with the orientation of the polarizer.

Cubes were cut from two GaAs ingots that had previously been characterized. The orientation of the faces of the cubes were selected to give a reasonable selection of the major crystallographic axes and are shown schematically in Figure 8. These were cut after X-ray orientation with all faces accurate to within ±1° of the directions shown in the Figure. The cubes were then processed as follows:

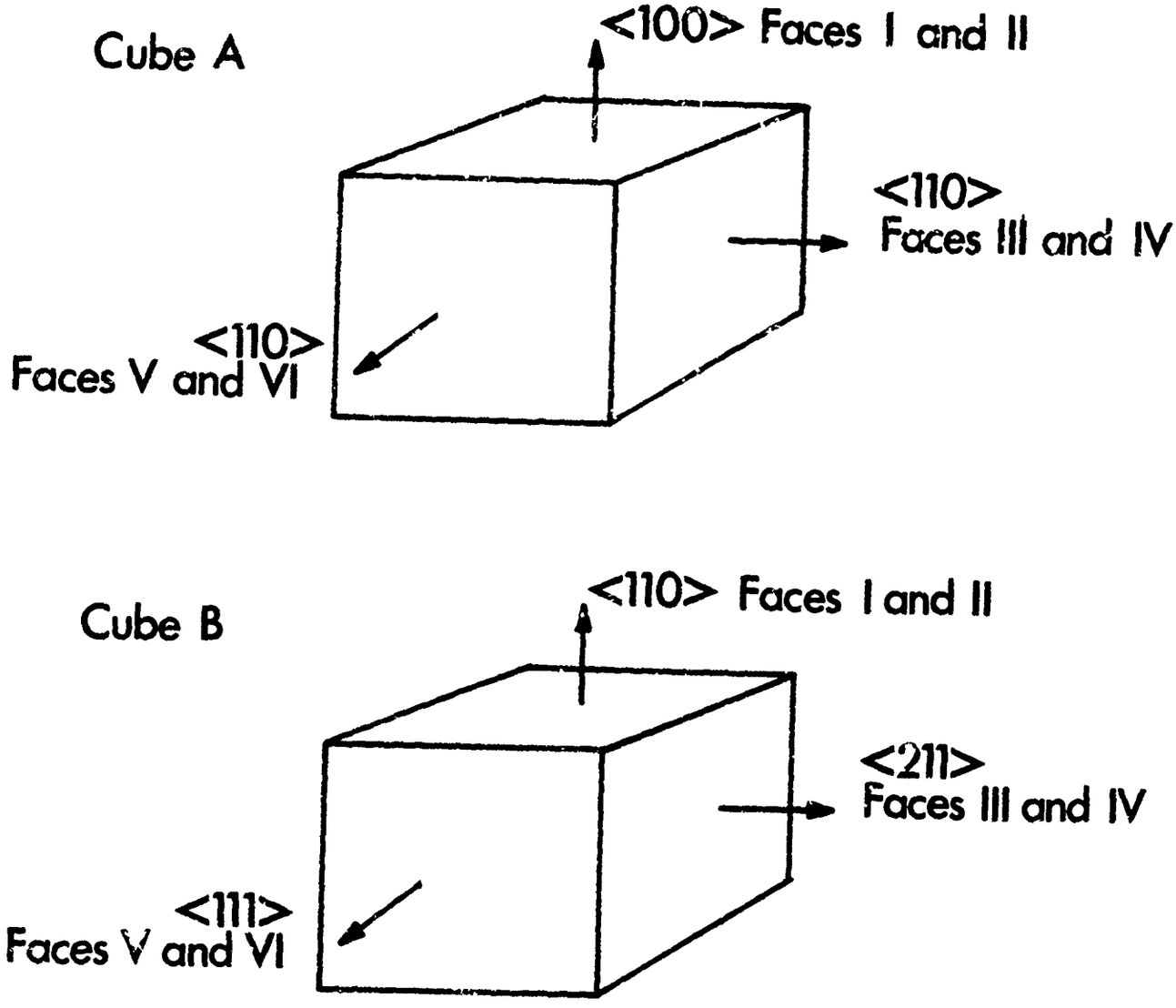


Figure 8. Schematic of GaAs Cubes Used to Test the Dependence of Absorption Coefficient on Crystallographic Directions

(a) All faces were lapped to a smooth finish and checked for orientation.

(b) Two opposite faces were polished (I and II) and measured for optical absorption from both directions and for the polarizer axis parallel to each side (four measurements in all).

(c) Two more faces were polished (III and IV) and the same measurements were made for each pair of faces (eight measurements).

(d) The final two faces were polished (V and VI) and the measurements repeated for the three pairs of faces (twelve measurements).

It was hoped that this combination would tell us what our reproducibility was under conditions of having most of the sample area "rough" through all of it polished, of mounting the sample on a polished or lapped face and under demounting, cleaning and remounting. The results are shown in Table 2. The variability $\Delta\alpha$ was computed by summing all the durations from the mean for each set of n measurements and dividing by $\sqrt{n}$. For cube A it was found there was no significant difference between steps in the processing, between polarization directions or between pairs of faces. It appears that the reproducibility is on the order of ±10% or better for a sample of this size. Due to the very small temperature differentials employed it is expected that the different radiation losses will be negligible. The same conclusions apply to cube B with the exception of faces V and VI which were {111} orientation. It is difficult to estimate the significance of those measurements since the difference between the two polarization directions was small. However, since this particular cube was higher in absorption it is probable that another effect is taking place. Absorption by microscopic gallium inclusions near either face V or face VI could have occurred since the beam was passed through the center and would miss this location for the other measurements. No such inclusions were seen on the evaluation slice taken below where the

TABLE 2

| Faces | | Cube A | | Cube B | |
|---|---|---|---|---|---|
| | | $\alpha$ | $\Delta\alpha$ | $\alpha$ | $\Delta\alpha$ |
| I and II | 2 faces polished | 0.0131 | 0.0011 | 0.0223 | 0.0029 |
| I and II | 4 faces polished | 0.0123 | 0.0007 | 0.0241 | 0.0067 |
| III and IV | | 0.0119 | 0.0013 | 0.0272 | 0.0007 |
| I and II | 6 faces polished | 0.0129 | 0.0008 | 0.0252 | 0.0065 |
| III and IV | | 0.0125 | 0.0006 | 0.0283 | 0.0030 |
| V and VI | | 0.0113 | 0.0011 | 0.0393 | 0.0024 |
| All I & II, Pol vertical | | 0.0129 | 0.0011 | 0.0248 | 0.0082 |
| All I & II, Pol horizontal | | 0.0126 | 0.0014 | 0.0243 | 0.0061 |
| All III & IV, Pol vertical | | 0.0124 | 0.0011 | 0.0283 | 0.0028 |
| All III & IV, Pol horizontal | | 0.0120 | 0.0010 | 0.0272 | 0.0009 |
| All V & VI, Pol vertical | | 0.0107 | 0.0008* | 0.0381 | 0.0006* |
| All V & VI, Pol horizontal | | 0.0118 | 0.0004* | 0.0405 | 0.0002* |

The absorption coefficients $\alpha$ of two cubes (see Figure 8) for all pairs of faces during processing (see text) and for polarization vector vertical and horizontal to the two sides of the face on which the laser beam is perpendicularly incident.

* Statistically insignificant - insufficient data.

cube was cut but this could have been a localized defect. This should be checked by making measurements on another cube incorporating {111} faces fabricated from low absorption material.

The major conclusion is that no differences in absorption coefficient were detected for two perpendicular polarization vectors incident on {100}, {110}, {111} or {211} faces.

4.5 Discussion of Results

The reproducibility of the laser absorption equipment was found to be 10% or better. We estimate the accuracy of our technique to be ±25% for GaAs. Comparison with other people's results is difficult due to the variability of the absorption coefficient from one sample to another. At the time of writing a round-robin is proceeding (organized by the Air Force/University of Dayton at Wright-Patterson Air Force Base). This involves a variety of materials and techniques and should do much to establish absolute values and define reproducible techniques. Two GaAs ingots supplied by us were kindly measured by Dr. T. Deutsch of Raytheon.[3] He obtained values of $\alpha$ via a dual beam spectrometric technique of $\sim 0.01$ cm$^{-1}$ for an Fe-doped sample and $0.005 \pm 0.003$ cm$^{-1}$ for a Cr-doped sample. We obtained a value with our calorimetric technique of 0.015 cm$^{-1}$ for the Fe-doped ingot. The Cr-doped ingot was not measured directly but ingots grown under similar conditions in the same period of time had $\alpha = 0.010 - 0.015$ cm$^{-1}$. The different techniques may be responsible for this difference, but it is possible that lower values than 0.01 cm$^{-1}$ are attainable for GaAs.

We have shown that a variety of surface treatments and sample sizes has an effect smaller than our experimental error on the optical absorption coefficient. There is an optimum range of chromium doping which is 1 to 4 ppma. The crystal growth axis and pull speed also have a negligible effect on the absorption coefficient for the values we tried. The resistivity of the sample has no effect providing it exceeds $\sim 10^6$ ohm-cm. Impurities at the

levels typically encountered also appear to have little effect but material obtained from non-stoichiometric melts which is purer and exhibits lower defect levels may lead to superior optical quality. No correlation could be found between the direction of a polarized laser beam and the crystallographic orientation on the absorption coefficient for the major crystallographic axes.

Further discussions on these results and a comparison with available theory can be found in Section 7.

# 5. LARGE DIAMETER GaAs

## 5.1 Large Diameter Czochralski Pulling

The size of a crystal that can be pulled from a melt by the Czochralski technique is limited by many factors including crucible size, vertical and horizontal gradients at the melt surface, heat flow through and radiation from the solidified ingot etc. Most of these factors are not known quantitatively, but their empirical effects on crystal growth are often known through experimentation for a given system and material. It is generally accepted that pulling ingots having a diameter greater than half the crucible internal diameter takes skill in setting up the correct gradients. In our case 3 cm diameter ingots are typically pulled from 6 cm internal diameter crucibles with good control over shape and exhibiting good yields. The pull weight and single crystal yield fall off as the ingot diameter is increased and the entire process becomes more critical.

Using this same system we pulled several ingots, two of which had good diameter control and diameters between 4.0 and 4.5 cm. Due to the factors mentioned above the pull weights were only 70% of the melt weight. Since this was a trial no attempts were made to optimize yields further. These ingots exhibited normal dislocation densities at the top (low $10^4 cm^{-2}$) but a greater tendency toward lineage at the bottom. Lowering the pull speed from 1.8 to 1.2 cm $hr^{-1}$ did not affect the results significantly. Optical absorption coefficients ranged from 0.010 $cm^{-1}$ to 0.023 $cm^{-1}$, the latter value corresponding to a sample with considerable lineage. It is felt that this size represents the maximum achievable with this particular crystal puller and the attainment of normal properties is an acceptable achievement.

In order to test the feasibility of extending the Czochralski technique to ingot diameters in the 7-8 cm range (for 3" diameter windows) the apparatus shown in Figure 9 was built. The crucible diameter was made approximately

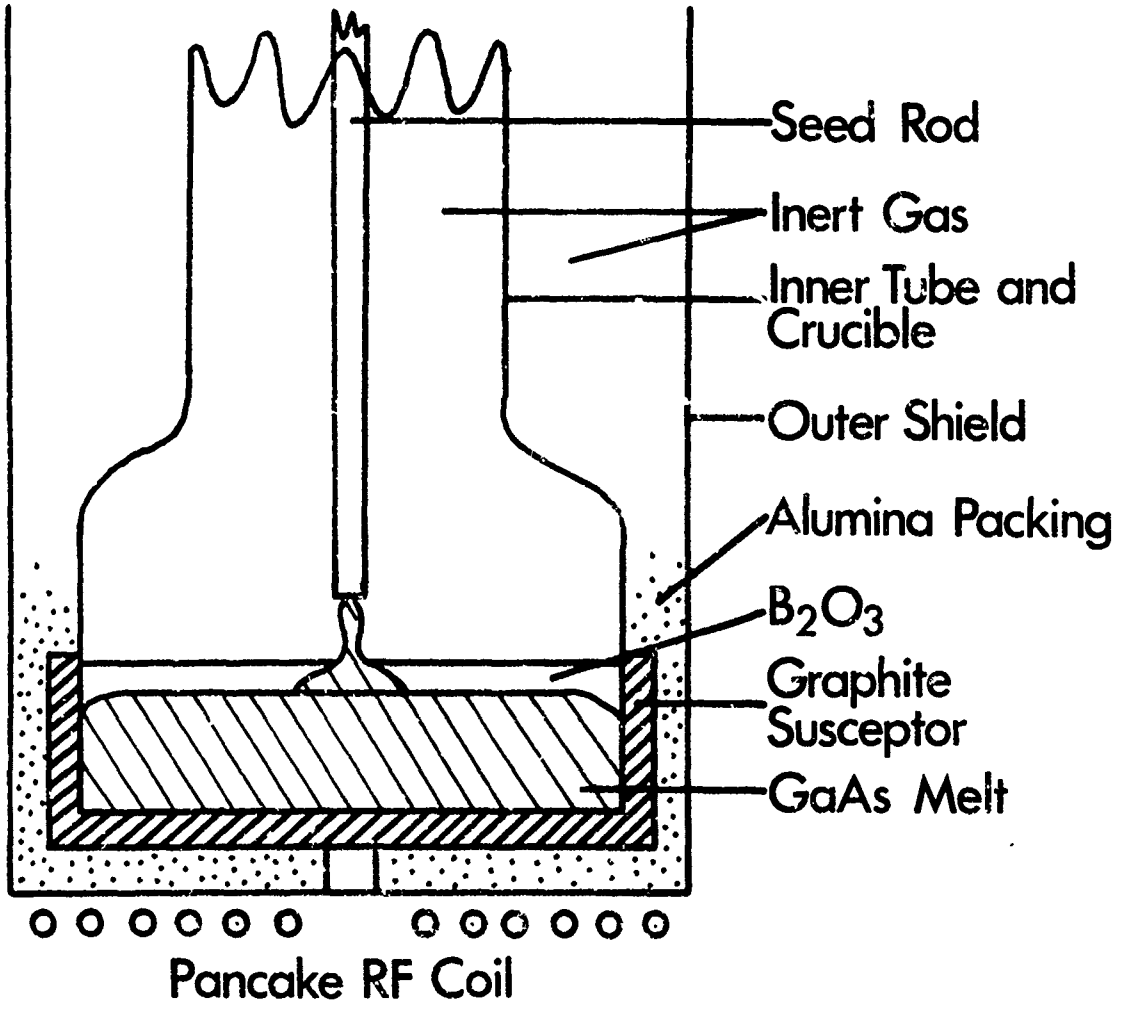


Figure 9. Schematic of Large Diameter Czochralski Apparatus

12 cm. To ensure uniform heating of such a large shallow melt a "pancake" coil was used (see Sub-section 5.3). The melt was liquid encapsulated and charge preparation, etc. was done in the manner normally used by us (as described in Sub-section 2.2). A <111>A oriented seed was used at a pull speed of 0.6 cm hour$^{-1}$. Difficulties were encountered with the strength of the quartz due to the weight of the charge (close to 1,500 gram) and the pressure on the bottom plate (~120 lbs from 10 psi inside the system). The glassware broke several times and the crucible plus susceptor tilted and slipped. The latter effect resulted in one side of the melt being ~100°C hotter than the other side which led to the growing ingot hitting a freezing portion growing from the cold side.

It was felt that the entire system would have to be rebuilt in order to strengthen it adequately, but time and money did not permit this. However, the seeding operation, the growth of a good-sized crown and degree of shape control experienced even under the above poor conditions were very positive signs that a design of this type could yield ingots having diameters in the 7-8 cm range.

## 5.2 Crucible Casting

This work started toward the end of the prior reporting period.[5] The intended approach was to control the freezing interface and move it slowly so that a directional solidification took place rather than the whole mass freezing at one time. The assembly used is shown in Figure 10. An internal diameter of 7.5 cm was selected as a reasonable compromise between a large increase over prior technology and keeping the charge weight at a safe and economical level.

The inner quartz container holds the melt of approximately 900 grams of GaAs. The outer container holds the graphite susceptor in place and cushions the inner container. also eases the pressure differential. The entire assembly is suspended from the seed rod of a crystal puller so that

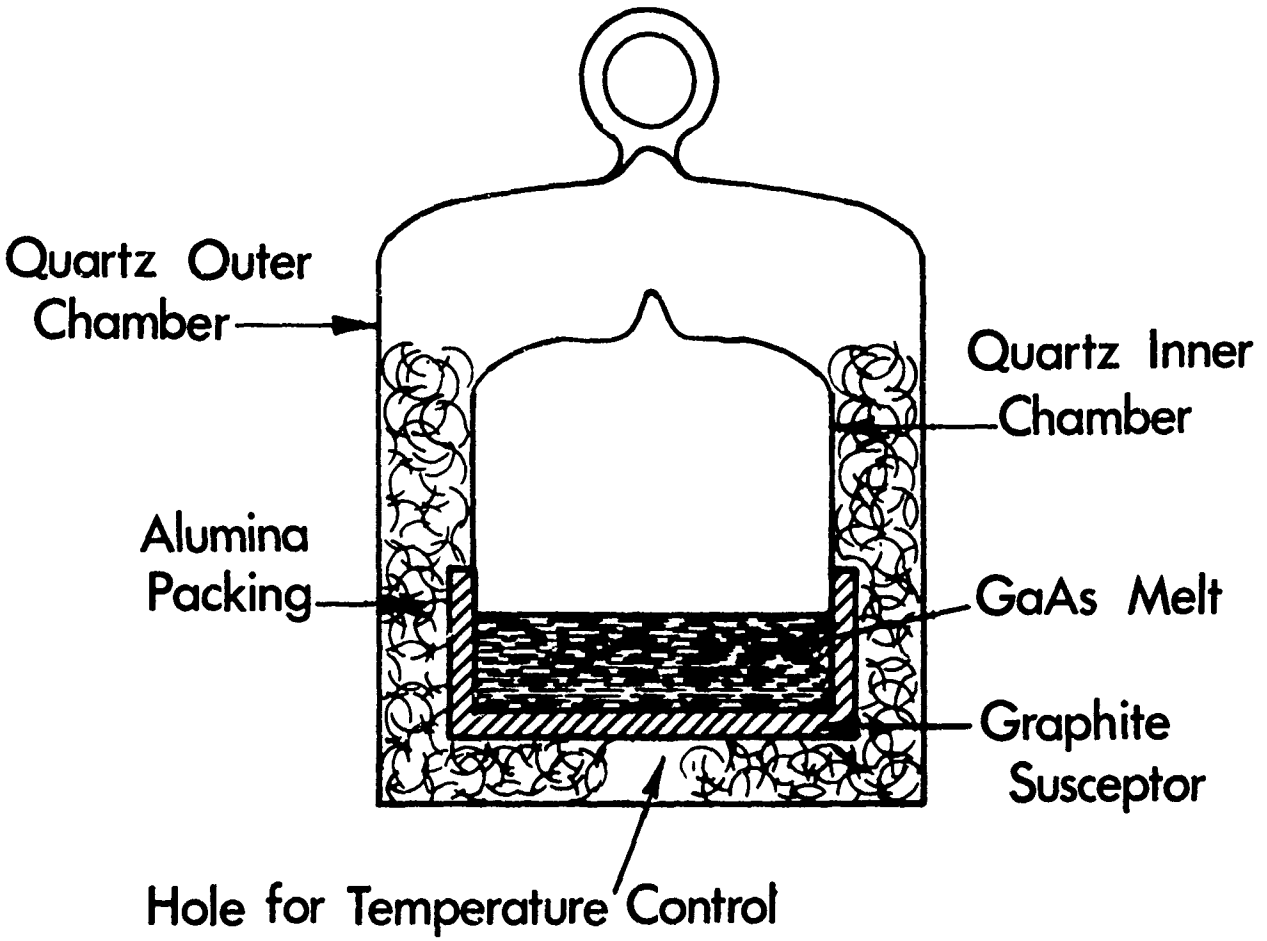


Figure 10. Method Used for Casting Large-Diameter Window Blanks

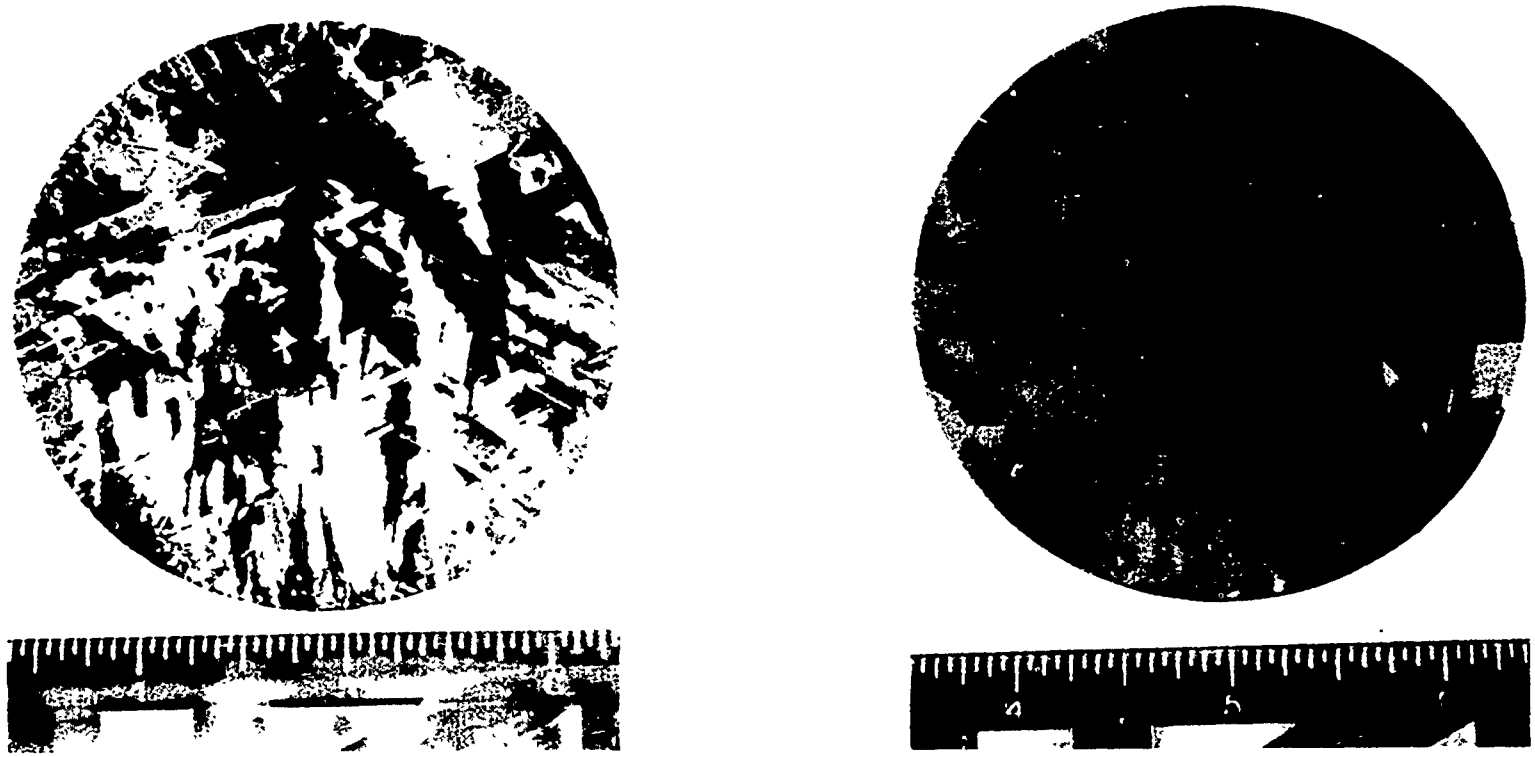

(a) (b)

Figure 10. Cross-sections of 3-inch Diameter Cast Boule of GaAs. (a) Rapidly Frozen Portion Near Top; (b) Large Grain Portion Near Bottom

it may be rotated and raised or lowered smoothly. With the susceptor located centrally in the RF coil the charge was melted and allowed to homogenize. With the surface of the melt, which is usually the coldest part, 20 °C above the freezing point the whole assembly was slowly lowered through the coil, thus causing the melt to freeze from the bottom upwards. It was found that the coldest part of the ampoule stayed above 610°C, assuring an adequate arsenic pressure. A rotation speed of 4 rpm was used with a lowering rate (which is approximately equal to the growth rate) of 1 cm $hr^{-1}$. The temperature of the melt surface had to be constantly monitored with the optical pyrometer since the coupling increases as freezing commences, and the power adjusted accordingly.

Cross sections from the top and bottom of a successful casting are shown in Figure 11. The top of this piece was obviously frozen rapidly and hence contains "blow-holes" and some gallium inclusions. However reasonably-sized grains are still visible. The first-to-freeze portion at the bottom has very nice grain structure with no evidence of inclusions, holes, etc. The largest grain has an area of well over 10 $cm^2$. This good polycrystalline growth persisted for about half of the boule depth until the rapid freezing commenced. Mass spectrometric results show a purity comparable with that of pulled material (see Sub-section 3.3). The optical absorption coefficient was measured on a thin piece cut from the bottom (first-to-freeze) portion and values between 0.03 and 0.11 $cm^{-1}$ were recorded. Examination with an infrared microscope showed the presence of small gallium inclusions, particularly at grain boundaries, thus explaining the high and variable absorption coefficient.

The main reasons for the presence of such inclusions as well as the porous material obtained in the last-to-freeze portion are lack of control over stoichiometry and the need to adjust power to compensate for the changing coupling between charge and RF coil which leads to rapid freezing rates

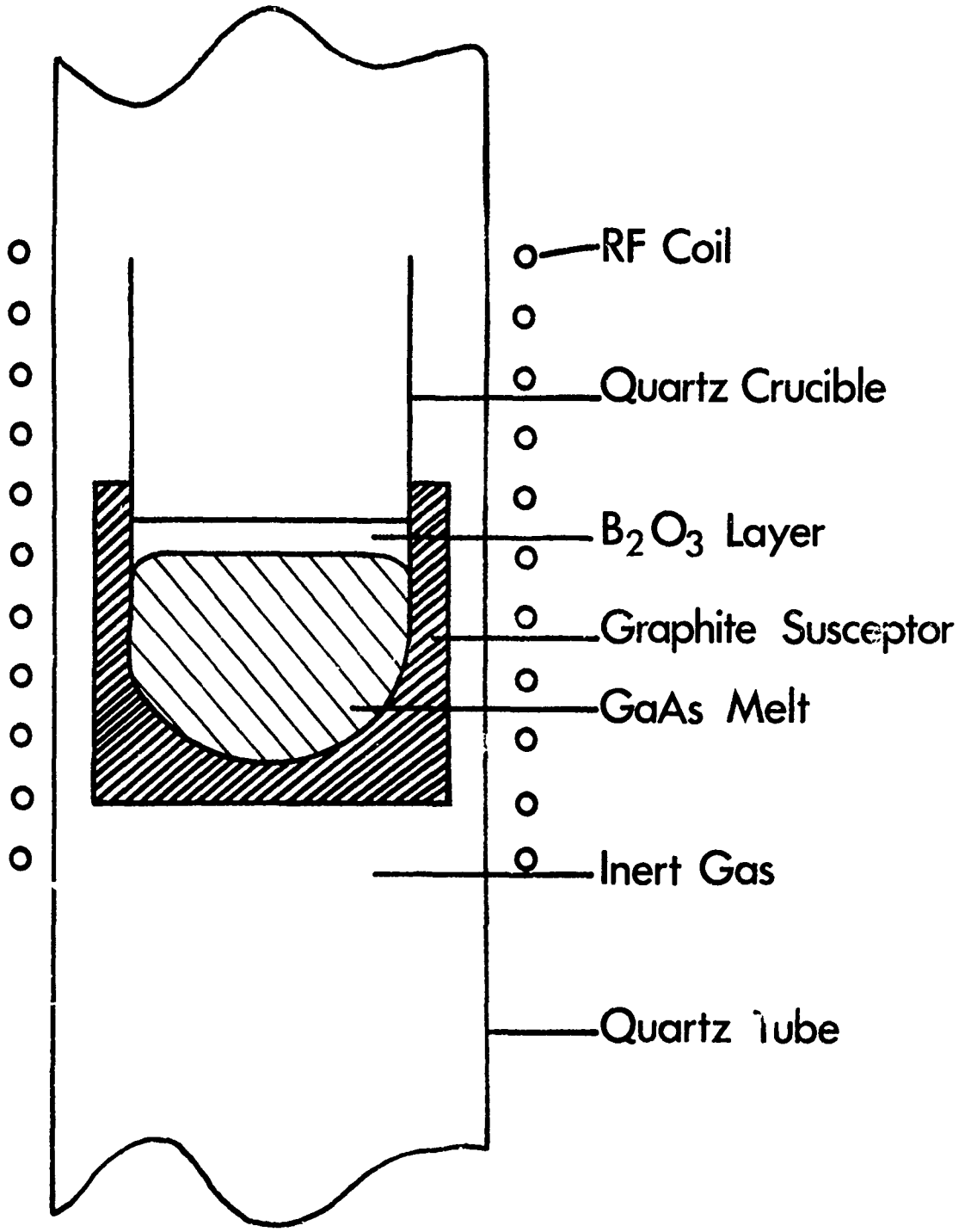


Figure 12. Schematic of Crucible Casting Technique

In an effort to overcome some of these difficulties the following experiments were performed.

Using the regular liquid encapsulation crystal puller an encapsulated charge of 700 grams in a 6 cm i.d. crucible was positioned in the lower half of the coil so that the bottom was colder than the top by 75-100 °C (measured from either end of the graphite susceptor). The layout is shown schematically in Figure 12. Three attempts were made with combinations of lowering and cooling at various speeds followed by slow cooling to room temperature. The crucible was rotated at 4 rpm during the entire run. All boules were cracked due partly to the solidifying layer of boric oxide which always cracks the quartz ampoule. Also they were extremely fine-grained and exhibited some inclusions and voids, indicating too rapid freezing interface movement.

A similar experiment was then performed except the $B_2O_3$ was left out and the charge was contained in a sealed ampoule, indicated by the dashed lines in Figure 12. Some of these ampoules partially collapsed during melt-down, drawing the quartz away from the susceptor leading to temperature inhomogeneities. This problem was overcome by backfilling with helium to an empirically determined partial pressure ($\sim$0.2 atm) and physically holding the ampoule in the graphite susceptor. Once again combinations of lowering the ampoule and slow cooling (calculated to give freezing rates of approximately 0.5 cm hour$^{-1}$) were tried. Rotation rates were as described above. Since temperature oscillations were experienced when the ampoule was low enough in the coil to give a reasonable gradient over the susceptor and these were magnified as the overall temperature fell. All boules were cracked to some extent and no large size grains were obtained, due largely to the inadequate temperature control achieved in the melt.

One of the better looking crucible castings was processed for spectral absorption measurements by cutting around the cracked portion. The absorption coefficient was found to vary drastically, values between 0.04 and

and 0.15 $cm^{-1}$ being observed, due to the presence of inclusions. This sample was worse under microscopic examination than the one described above which correlates well with the optical results.

In order to test this technique fairly two major changes would have to be made. Stoichiometry can be controlled by using an excess of arsenic and extending the ampoule vertically and employing a separate resistance furnace and with the coldest part at ~620°C. The temperature control problem could be overcome by controlling the power to the RF coil via a pickup on the input leads rather than via a temperature sensor which is viewing the bottom of the susceptor. It is probable that such improvements would make this a useful and relatively easy technique for producing boules in the 5-7 cm diameter range. However, extension to much larger sizes would be fraught with problems and therefore another approach was adopted which will be described in the next sub-section.

## 5.3 Radial Casting

Both the Czochralski and Crucible Casting Techniques have disadvantages which become severe when an extension to 25 cm diameter boules is considered. With these disadvantages in mind and with the experience of practical difficulties encountered a third technique was devised which we have chosen to call Radial Casting. The limiting factor of the methods described in subsections 5.1 and 5.2 is that of interface stability—in all cases a large area will tend to go into oscillations which results in rapid freezing and melting. This leads to voids, inclusions and generally poor crystallinity. Figure 13 shows the types of interface shapes involved. For boule sizes ~7.5 cm diameter we have a curved area of approximately 50 $cm^2$ and as the diameter increases this area goes up as the square of the diameter. Also the center of the area gets further from the source of heat and the heat loss mechanisms, which is the cause of the instabilities (via local supercooling) mentioned above.

The radial casting technique utilizes a shallow melt in a circular

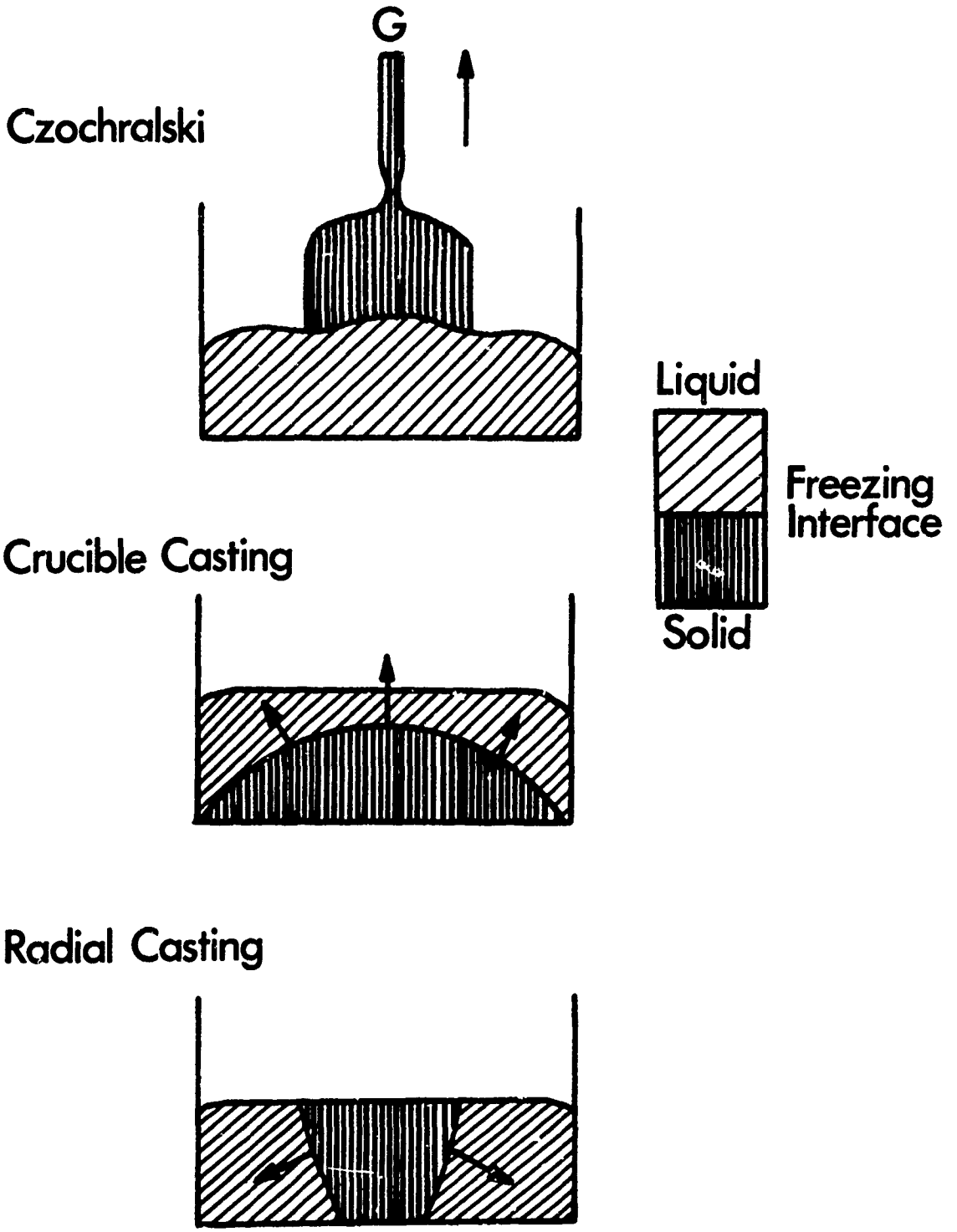


Figure 13. Comparison of Liquid-Solid Interface Shapes for Three Techniques

crucible. A temperature gradient is arranged so that the center is cooler than the circumference. By lowering the temperaturature the melt will freeze from the center outward at a directly controllable rate, much as a gradient freeze furnace works for boat-grown material. Here the solid liquid interface starts off small and as the diameter increases its maximum size only increases directly proportionally to the diameter, not as the square. The heating and heat loss mechanisms at all times are close to all parts of this interface ensuring a narrow circular strip shape which is stable. By arranging the heating correctly the top can be made slightly colder than the bottom giving an interface shape similar to that shown in Figure 13; this is desirable so that freezing is initiated from a free surface rather than a crucible wall. It is conceivable that seeding could be carried out in the center resulting in a single crystal disc. Lastly, the finished casting is in the shape and size required for a laser window and only grinding and polishing operations would be required.

Figure 14 shows a schematic of the equipment built to test the possibility of radial casting and to learn of the type of practical problems that might occur during scale up. A pancake RF coil was used with the turns spaced to give a radial gradient with the circumference being hotter than the center as sketched in Figure 14. The quartz outer shield was flushed with argon and a small flow continued throughout the run to prevent serious erosion of the graphite susceptor. The crucible diameter was 7.5 cm and the melt size was varied between 400 and 500 grams. The ampoule collapsing or bulging problems experienced with the crucible casting technique were again observed and partially overcome in the manner described in sub-section 5.2.

Out of several attempts one run gave good material without obvious voids or cracking. A photograph of the cross section of this boule is shown in Figure 15. The dopant level was inadequate to give high resistivity due to a calculation error and an absorption coefficient was therefore not obtained.

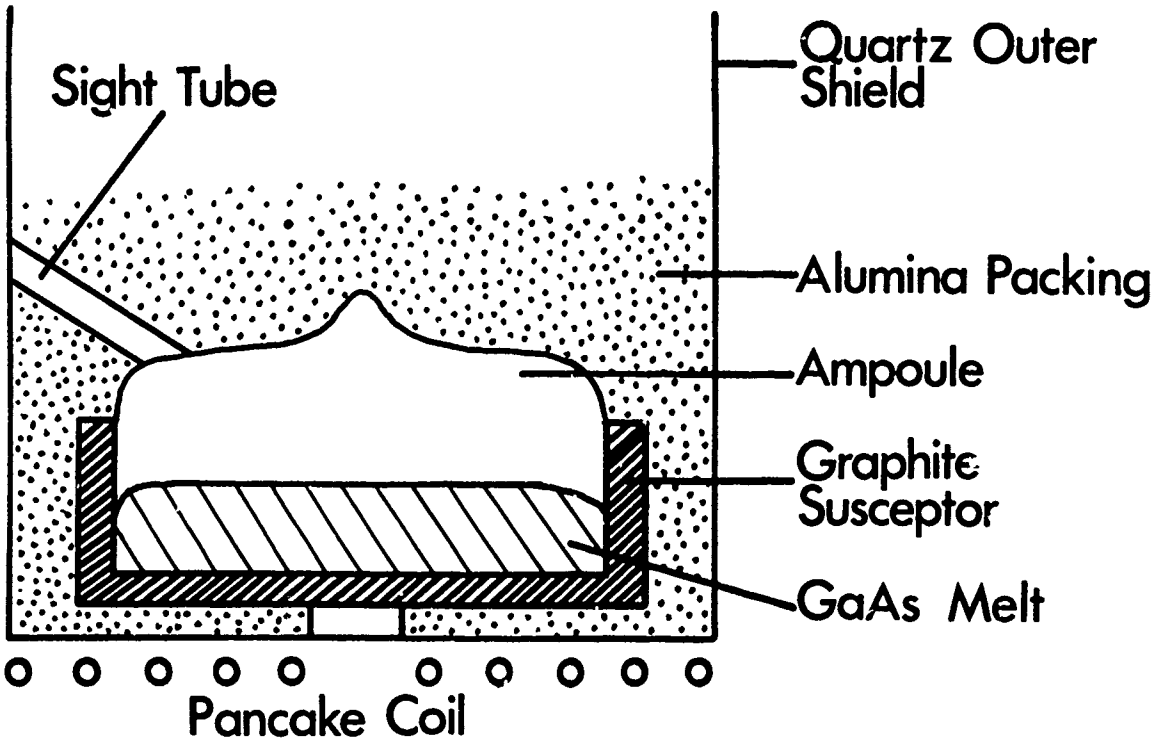


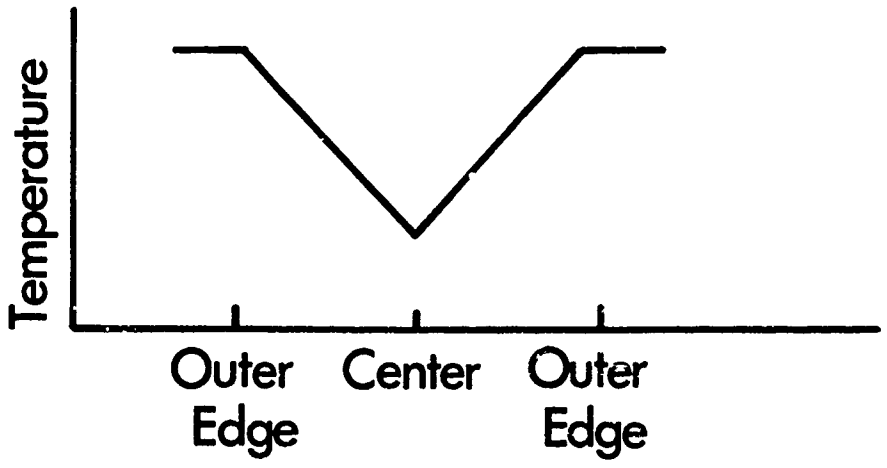


Figure 14. Schematic of Radial Casting Technique and Temperature Profile Employed


Figure 15. Cross Section of Three-inch Diameter Radially Cast Boule

The grain structure shows growth initiating from close to the center and proceeding outwards as planned with large grain size generally evident. The coil shape and spacing would have to be adjusted slightly to give growth initiation at the center and an equal growth speed in all directions.

## 5.4 Discussion of Results

Three major techniques were tried and the following conclusions can be drawn.

The large-diameter Czochralski technique should be feasible with a stronger apparatus. The vertical and horizontal gradients looked excellent and no trouble was experienced in controlling the melt temperature and mechanical stability. This technique will prove most useful for producing single crystal GaAs ingots from which window blanks 4 to 8 cm in diameter can be processed. Other shapes for beam-splitting or Brewster window applications having a minimum dimension in the same range could also be cut from such ingots.

The crucible casting would appear to be an excellent choice for relatively inexpensive windows in the 5 to 7 cm range as long as polycrystallinity is no problem in the final application. Here the design we employed would be changed in detail but not drastically. The "cold" end of the closed ampoule should be controlled by a resistance heater to maintain the required stoichiometry while the power level from the RF generator to the melt should be controlled either by a pickup coil on the input or the temperature of the melt surface. Since the latter is usually difficult to achieve in a practical system the former would be the best technique.

The radial casting offers the greatest promise for diameters of 7 to 10 cm and beyond. Again the stoichiometry should be controlled by controlling the temperature of the cold end of the ampoule. Our particular equipment would also have to be strengthened and coil spacing, etc. optimized. In the

larger sizes the temperature of the periphery might become excessive but good control over the temperature gradient should minimize this effect at least for diameters to 25 cm. Thicker windows might require a second pancake coil above the melt as well as below it with an enveloping graphite susceptor but the heat loss from the free surface can be controlled to a great extent by heat reflecting material placed close to it. Lastly, the potential of obtaining single crystal blanks is possibly the most attractive point of this novel technique.

## 6. PREPARATION AND PROPERTIES OF GaSb

Gallium antimonide is the second of the III-V compounds that meets the criteria stated in Section 1 of this report. It has a bandgap ~0.75 eV which is borderline and would render the material unsuitable for operation at temperatures exceeding typical ambients. However, because Sb is much heavier than As, the phonon frequencies of GaSb are smaller and therefore at longer wavelengths than those of GaAs. It is possible therefore that if the 10.6 μm optical absorption coefficient is due to multiple phonon bands then it will be lower in GaSb than in GaAs. Since GaSb had not previously been prepared in high-resistivity form our first efforts lay in investigating the electrical behavior of the material under different doping conditions.

The preparation of the material has been described in detail previously.[5] Most of the results discussed here were obtained on ingots pulled from melts whose stoichiometry varied from 50 at % Sb to 70 at % Sb; liquid encapsulation was used for only a few of the attempts. The electrical results are summarized in Figure 16 which shows the variation of carrier concentration at 300 °K and 77 °K in undoped material as a function of initial melt stoichiometry. Good agreement was obtained with the results of Reid, et al.[26] The mobilities we observed ranged up to 5,500 $cm^2 V^{-1} sec^{-1}$ at 77 °K for an ingot pulled from a 70 at % Sb melt. Chromium was tried as a deep level dopant on both p-type and n-type (Te doped) material. Although the amount of chromium averaged around 4 ppma no high resistivity material was obtained. The electrical properties of these ingots are difficult to interpret simply, but they are basically n-type with low mobility- the "best" ingot had a resistivity ~ 1 ohm-cm. Due to the mixed conduction a multi-band Hall analysis would be needed to obtain more information on the carrier concentrations, but since the resistivity is the critical parameter here a combination of simple Hall effect and mass spectrometric analysis was deemed sufficient.

At this time in the program the GaAs effort took on additional

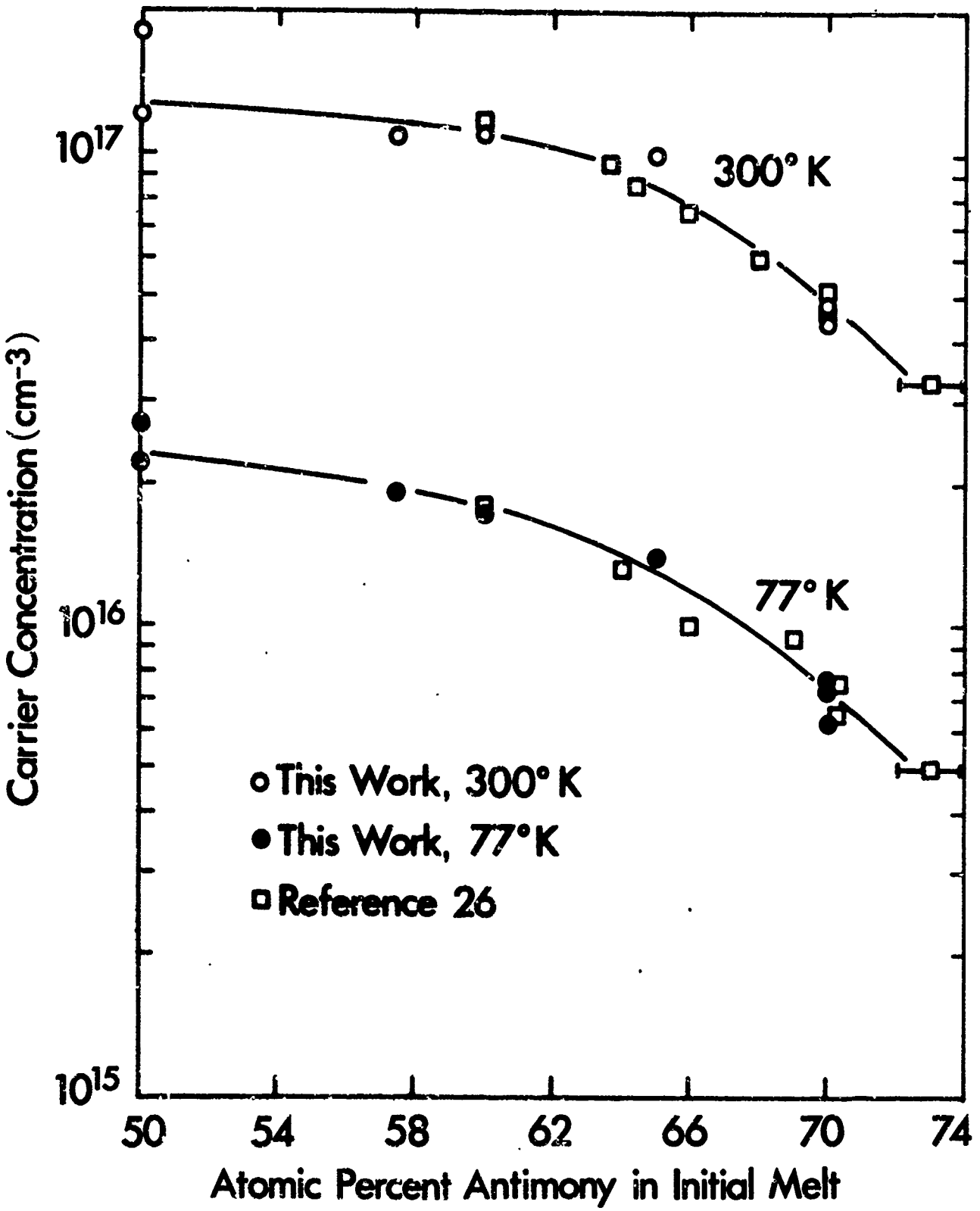


Figure 16. The Carrier Concentration in Undoped GaSb at 300°K and 77°K as a Function of the Stoichiometry of the Melt

importance and so no further work was performed. It should be possible to grow high resistivity GaSb by keeping the intrinsic carrier concentrations low by growing from non-stoichiometric melts, probably using n-type material and surveying the type of dopants that have been found to give deep levels in other III-V compounds.

# 7. CONCLUSIONS

## 7.1 Discussion

This work has covered a wide spectrum of experimental investigation. It has been shown that GaAs can be reproducibly prepared with an absorption coefficient below 0.02 $cm^{-1}$ at 10.6 μm and the properties necessary for this to occur have been discussed in some detail. The lowest absorption coefficients seen by us on our material were ~0.009 $cm^{-1}$; others obtained values as low as 0.005 $cm^{-1}$ with Cr-doped GaAs prepared by us. The role of defects of the vacancy type has not yet been clarified but the initial results on ingots pulled from non-stoichiometric melts look promising. No polarization dependence of the absorption coefficient could be found but the results are not completely conclusive.

Three different techniques were proposed and tried for the preparation of large diameter GaAs. For single crystal material in the 4-8cm diameter range, Czochralski pulling should be used; for polycrystalline material in the same range crucible casting offers simpler equipment and some cost saving. For larger diameters the novel technique of radial casting proved successful. It is anticipated that with relatively minor modifications this technique could be used to prepare windows up to 25 cm in diameter. There is also a possibility of preparing single crystal material in the same diameter range with this technique.

The results on GaSb were inconclusive because the best material had too low a resistivity (~1 ohm-cm) to permit optical measurements.

In view of the consistency of the optical absorption coefficient failing to fall significantly below ~0.01 $cm^{-1}$ it is of interest to examine the theory of optical absorption in GaAs. This point was briefly discussed in Sections 1 and 4.1 of this report. In particular Sparks[22] has given an excellent elementary introduction into some of the types of processes that contribute

to the absorption of photons in this wavelength region. It is apparent that much work remains to be done to develop a quantitative theory. The attempts that have been made to date[20,21,27] have tried to fit the phonon-band region data with some success but the shorter wavelength region has either been neglected completely or higher-order effects which affect this region have not been taken into account.[27]

We feel that a theoretical investigation is sorely needed to establish a probable value for the optical absorption coefficient in GaAs and other semiconductors. Such an investigation would be aided by extensive data concerning the variation of the experimental absorption coefficient with wavelength (from the absorption edge out into the multiphonon bands) and temperature.[22]

## 7.2 Future Work

The initiation of a combined theoretical and experimental investigation into the fundamental causes of absorption should have a high priority. The work now being done by Haggerty et al[19] on our material may find some of the cause of the variation in absorption coefficient we have observed besides the effects discussed in sub-section 7.1. The effects of defect level should also be studied in more detail.

As was suggested in Section 5 the three large diameter techniques are each of interest for different final applications. Very little additional work would be required to put any one of these on a routine basis. This would represent a significant advance in size over the material currently available by more traditional means, thus satisfying the major aim of this work.

## 8. ACKNOWLEDGMENTS

The author wishes to acknowledge the invaluable assistance rendered by R. K. Willardson, J. W. Wagner and D. R. Nichols of this laboratory. The mass spectrometric analyses were ably performed by E. M. Masumoto. The competent and enthusiastic technical assistance of F. Hicklin, K. Schwartz and T. Tench is gratefully recognized. Discussions held with R. Rudko and T. Deutsch of Raytheon Research Division, J. Kiefer of Hughes Research Laboratories and J. S. Haggerty of A. D. Little Company have proved useful. The direction and suggestions supplied by V. O. Nicolai were essential to the successful completion of this work.

## 9. REFERENCES


1. R. I. Rudko and F. A. Horrigan, AD 693 311 (September, 1969).

2. F. Horrigan, C. Klein, R. Rudko and D. Wilson, Microwaves, p. 68 (Jan. 1969).

3. F. Horrigan, T. F. Deutsch, Final Tech. Rpt., Contract #DAAH01-70-C-1251 (Sept. 1971).

4. J. S. Jasperse and P. D. Gianino, J. Appl. Phys 43, 1686 (1972).

5. A. G. Thompson, AD 720 390 (December, 1970).

6. E. P. A. Metz, R. C. Miller and R. Mazelsky, J. Appl. Phys. 33, 2016 (1962).

7. J. B. Mullin, B. W. Straugham and W. S. Brickell, J. Phys. Chem. Solids 26, 782 (1965).

8. J. W. Wagner and R. K. Willardson, Trans. Met. Soc. AIME 242, 366 (1968).

9. A. R. Von Neida, L. J. Oster and J. W. Nielsen, J. Cryst. Growth 13-14, 647 (1972).

10. A. G. Thompson and J. W. Wagner, J. Phys. Chem. Solids 32, 2613 (1971).

11. J. W. Wagner and R. K. Willardson, Trans. Met. Soc. AIME 245, 461 (1969).

12. G. R. Cronin and R. W. Haisty, J. Electrochem. Soc. 111, 874 (1964).

13. O. Madelung, "Physics of III-V Compounds," Wiley, New York, p. 263 (1964).

14. J. Blanc and L. R. Weisberg, Nature 192, 155 (1961).

15. R. K. Willardson and W. P. Allred, Proc. of First Intl. Symp. on GaAs at Reading, p. 35 (1966), (Inst. of Phys. and Phys. Soc., London, 1967).

16. W. DeVilbiss, Ph.D. Thesis, U. of Missouri, Columbia, (1968).

17. T. Inoue and M. Ohyama, Solid State Comm. 8, 1309 (1970).

18. E. D. Jungbluth, Metall. Trans. 1, 575 (1970).

19. J. S. Haggerty and E. T. Peters, AD 740 207 (March, 1972).

20. "Semiconductors and Semimetals," R. K. Willardson and A. C. Beer, Eds., Vol. 3, (Academic Press, New York, 1967).

21. W. Cochran, S. J. Fray, F. A. Johnson, J. E. Quarrington and N. Williams, J. Appl. Phys. 32, 2102 (1961).

22. M. Sparks, Quarterly Tech. Progr. Rept. #1, Contract #DAHC15-72-C-0129 (March, 1972).

23. V. O. Nicolai and G. W. Gottlieb, AD 859 306 (1969).

24. R. Weil, J. Appl. Phys. 41, 3012 (1970).

25. V. O. Nicolai, Private communication (1972).

26. F. J. Reid, R. D. Baxter and S. E. Miller, J. Electrochem. Soc 113, 713 (1966).

27. H. Borik, Phys. Stat. Sol. 39, 145 (1970).